Research papers

The 3DNet-Catch Hydrologic Model: Development and Evaluation

Andrijana Todorović, Miloš Stanić, Željko Vasilić, Jasna Plavšić

PII: S0022-1694(18)30802-3
DOI: https://doi.org/10.1016/j.jhydrol.2018.10.040
Reference: HYDROL 23204

To appear in: *Journal of Hydrology*

Received Date: 10 June 2018
Revised Date: 10 September 2018
Accepted Date: 17 October 2018

Please cite this article as: Todorović, A., Stanić, M., Vasilić, Z., Plavšić, J., The 3DNet-Catch Hydrologic Model: Development and Evaluation, *Journal of Hydrology* (2018), doi: https://doi.org/10.1016/j.jhydrol.2018.10.040

The 3DNet-Catch Hydrologic Model: Development and Evaluation

Short title: The 3DNet-Catch Hydrologic Model

Andrijana Todorović[a*], Miloš Stanić[a], Željko Vasilić[a], Jasna Plavšić[a]

[a] University of Belgrade, Faculty of Civil Engineering, Bulevar kralja Aleksandra 73, Belgrade, Serbia

[*] Corresponding author, e-mail: *atodorovic@grf.bg.ac.rs*

Abstract

Hydrologic models are important for effective water resources management. They vary in complexity from parsimonious, spatially lumped, to physically-based, fully distributed models, which are generally expected to outperform the former. Wide applications of complex models are limited due to high data and computational demands. Therefore, a new approach based on well-balanced model complexity is needed to obtain reasonable simulation results with low data requirements. This paper presents a novel 3DNet-Catch hydrologic model, developed to represent key processes in sloped catchments under a temperate climate with modest data requirements. 3DNet-Catch includes runoff simulations within computational units by employing the interception, snow and soil routines, as well as runoff and channel routing. The soil routine, which is the key model feature, combines the SCS-CN method, an analytically integrated nonlinear outflow equation and the Brooks-Corey relation for unsaturated conductivity in an innovative manner. To advance runoff routing in 3DNet-Catch, an approach for analytical integration of the linear and nonlinear outflow equations is implemented. Most model parameters are physically meaningful, thus facilitating model calibration. The model structure can be adjusted according to soil and groundwater flow data, and it can include hydraulic structures, thereby providing adaptability to local conditions. A comprehensive hydrologic evaluation framework is established and conducted to examine whether 3DNet-Catch is adequately parameterised and can accurately reproduce catchment hydrologic response. The model parameterisation is evaluated by sensitivity, identifiability and correlation analyses. Model efficiency is quantified in terms of performance measures, hydrologic signatures and plausibility of the simulated hydrological processes. The results show high sensitivity of the hydrologic variables and performance measures to the model parameters, particularly to those of the soil routine. The parameters are uncorrelated and generally well identifiable. The model performs equally well in the calibration and evaluation periods. High efficiency in the hydrological signatures related to the soil routine indicates its robustness. The results, therefore, suggest that 3DNet-Catch is a comprehensively parameterised, versatile hydrologic model. It realistically reproduces observed hydrographs with modest data requirements, thus being appropriate for both engineering applications and investigative catchment dynamics studies.

Keywords

3DNet-Catch; conceptual hydrologic models; continuous hydrologic simulations; model parameterisation; robust model evaluation framework; soil routine.

Nomenclature

α – precipitation gradient with elevation

A – drainage area

A_b – baseflow drainage area

alpha – ratio between standard deviation of the simulated and observed series

B – maximum baseflow rate

b_{melt} – melt (degree-day) factor

$b_{melt,6}$ – melt factor on 21st of June

b_{melt} – melt factor on 21st December

c – nonlinearity coefficient of the groundwater reservoir

CAN – capacity of the canopy reservoir

CN – surve number

cov_{soil} – soil cover index

CU – computational unit

D – thickness of a soil layer

Δt – time step

E_{can} – evaporation from canopy

E_{soil} – bare soil evaporation

E_{sub} – snowpack sublimation

E_t – transpiration

FC – soil layer storage at field capacity

I_a – initial abstraction

K – vertical hydraulic conductivity

K_d – coefficient of the surface runoff linear reservoir

KGE – Kling-Gupta efficiency

KGE_{logQ} – Kling-Gupta efficiency for log-transformed flows

$K_{gw\text{-}fast}$ – coefficient of the linear reservoir for fast groundwater discharge routing

KS – Kolmogorov-Smirnov test

λ – snowpack temperature lag factor

LAI – Leaf Area Index

M – snowmelt (water equivalent)

n – pore-size distribution index

N_L – number of soil layers

NLGW – nonlinear groundwater reservoir

NSE – Nash-Sutcliffe efficiency

p – effective soil porosity

P – precipitation

P' – precipitation and/or throughfall

PET – potential evapotranspiration

P_S – snowfall

PWP – soil layer storage at permanent wilting point

Q – flow

Q_b – baseflow

q_d – maximum specific baseflow yield

Q_d – direct runoff

Q_{gw_fast} – fast groundwater discharge

q_{surf} – surface runoff per unit area

Q_{surf} – surface runoff from entire drainage area

r – Pearson correlation coefficient

R – throughfall

R^2 – coefficient of determination

s – share of a soil layer in the active soil zone

S_b – storage of the NLGW reservoir

S_{can} – canopy reservoir storage

S_d – storage of the surface runoff linear reservoir

S_{max} – threshold of the NLGW reservoir

s_{max} – the value of S_{max} per unit area

$\mathrm{S}_{s,max}$ – potential soil retention at permanent wilting point

$S_{s,max}$ – potential soil retention at field capacity

S_r – effective soil saturation

S_{snow} – snowpack storage

$S_{snow,100}$ – threshold snowpack storage at which the entire computational unit is covered in snow

STO – capacity of the soil layer, which is a product of soil porosity and the layer thickness

SW –storage of a soil layer

SWC – soil water content

θ_{FC} – soil water content at field capacity

θ_{PWP} – soil water content at permanent wilting point

T – air temperature

T_{lapse} – temperature lapse rate

T_{melt} – snowmelt temperature

$T_{R\text{-}S}$ – discrimination temperature between rainfall and snowfall

T_s – temperature of the snowpack

V_b – baseflow volume over a time step

VE – volumetric efficiency

V_{perc} – percolation volume over a time step

w_{perc} – percolation for a soil layer

1. Introduction

Hydrologic (rainfall-runoff) models are widely applied for estimation of design flows, flow forecasting, assessment of climate change impacts or various water management scenarios (Beven, 2001a). Being so important for water resources management, these models are required to provide accurate simulation results under various hydrologic conditions, preferably with low data and computational requirements. Presently, there are numerous hydrologic models that vary in complexity from parsimonious ones, like GR2M (Perrin et al., 2001), *abcd* (Thomas, 1981) or HYMOD (Boyle et al., 2001), to complex, fully distributed models, such as PIHM (Qu and Duffy, 2007), tRIBS (Ivanov et al., 2004) or MIKE-SHE (Refsgaard and Storm, 1995). The former, so-called conceptual models provide an abstract representation of runoff generation, which involves storage elements and simplified relations that describe water transfers among them (e.g., Mendoza et al., 2014). There is a wide variety of conceptual models and some of them have quite elaborate structures with numerous components. Physically-based models rely on explicit descriptions of hydrological processes with differential equations grounded in the conservation laws that have to be solved numerically (Hrachowitz and Clark, 2017). Unlike these two modelling approaches, data-driven (black-box) models, such as those based on neural networks, do not consider runoff generation processes (Pechlivanidis et al., 2011). Regardless of their complexity, hydrologic models are always simplified representations of catchment processes.

Model complexity can be analysed with respect to: (1) model structure, (2) methods employed or (3) spatial resolution. In terms of model structure, many hydrologic models omit a snow routine (Kauffeldt et al., 2016). The original version of the HBV model (Bergström and Frosman, 1973) did not comprise an interception routine, which was incorporated in subsequent model versions to obtain more realistic model (Lindström et al., 1997). This enhancement improved performance of the HBV model in some catchments, as demonstrated by Fenicia et al. (2008). The interception routine is also left out in some complex physically-based models, such as CATHY (Sulis et al., 2012) or HYDRUS (Šimůnek et al., 2009). Most hydrologic models do not simulate groundwater-surface interactions; hence, they cannot accurately reproduce unsaturated zone dynamics in lowland catchments (Brauer et al., 2014). In spatially lumped models runoff routing is based on arbitrary transfer functions, such as a triangular weighting function included in the HBV-type models (Schaefli et al., 2014).

Some hydrological processes can be described in a simple manner, even in complex models. For example, KINEROS (Woolhiser et al., 1990), MIKE-SHE, PREVAH (Viviroli et al., 2009), SWAT (Neitsch et al., 2011) and VIC (Liang et al., 1994) use simple canopy methods. Snow routines in many complex models (e.g., PIHM) are based on the simple degree-day method. Few other models, such as ARNO (Todini, 1996), PRMS (Markstrom et al., 2015) or VIC include robust energy budget-based methods. Soil water content (SWC) in conceptual models is usually simulated by employing simple methods. For example, some models assume a constant percolation rate (e.g., HBV), while in others, such as ARNO, GR4J (Perrin et al., 2003), LISFLOOD (Van Der Knijff et al., 2010), SEHR-ECHO (Schaefli et al., 2014), SIMHYD (Chiew et al., 2010) or WetSpa (Shafii and Smedt, 2009) percolation is expressed as a function of the SWC.

Greater model complexity usually implies an increase in the number of free parameters. Parameters of the physically-based models generally have a physical meaning and can be inferred from data on land-use, soil, vegetation and geology. However, some parameter adjustment is still required to achieve the best fit to the observations (Beven, 2001b). This is a challenging task because many parameters have to be estimated against few observed variables. Specifically, model calibration is usually performed against observed flows only, and information contained in the observed flows series allows identification of up to four parameters (Jakeman and Hornberger, 1993). Therefore, calibration of complex models is an ill-posed optimisation problem (Ebel and Loague, 2006), which leads to low parameter identifiability and equifinality that amplifies with the number of parameters (Beven and Binly, 1992).

Distributed models can capture spatial variability of catchment properties, meteorological and hydrologic variables, and can simulate various spatial runoff components (Schuurmans and Bierkens, 2007). These models generally provide higher efficiency than the lumped ones (Chang and Chao, 2014), but they are computationally and data demanding (i.e., they require high-quality input data).

A general assumption is that complex models yield realistic simulation results, i.e., that they provide "right answers for the right reasons" (Kirchner, 2006). These models are, therefore, expected to outperform parsimonious ones (Wagener et al., 2003), especially under conditions different from those encountered in the calibration period (Kuczera and Parent, 1998). However, examples of the opposite behaviour can be found in the literature: for example, simple models can result in lower decrease in model performance over evaluation periods than complex models, probably due to the over-parametrisation of the latter (e.g., Perrin et al., 2001; Orth et al., 2015). Furthermore, Orth et al. (2015) reported that a simple model outperformed two models with more complex structures during dry periods. Therefore, complex, fully distributed models are not necessarily the best choice. Moreover, model selection depends on data availability and specific application needs (Hrachowitz and Clark, 2017). For example, parsimonious models can be suitable for simulations in large catchments with long (e.g., monthly) time steps (van Esse et al., 2013).

To obtain realistic simulation results with low data and computational requirements, a model with well-balanced structural complexity is needed. The model structure should be sufficiently complex to replicate the key runoff generation processes, and thereby capture nonlinear and nonadditive catchment behaviour (Kirchner, 2006). Preferably, the model should be easily adaptable to local conditions

(Mendoza et al., 2014). This is in line with recommendations made by Seibert and McDonnell (2002), who suggested the use of "soft data" on catchment behaviour (i.e., qualitative knowledge). Additionally, a model should be able to represent various river engineering interventions (e.g., reservoirs, diversions) and changing land use. Presently, few models, such as HEC-HMS (Feldman, 2000), HYPE (Lindström et al., 2010), MIKE-SHE or TOPKAPI (Ciarapica and Todini, 2002), can integrate hydraulic structures. Urbanised areas, which are usually regarded as impervious zones (e.g., ARNO, HEC-HMS, LISFLOOD, PRMS), are also often disregarded.

To ensure suitability to local conditions, some models were specifically developed to reflect prevailing runoff processes in particular regions. For example, WaSiM-ETH (Schulla, 2017), SEHR-ECHO or PREVAH were developed for Alpine catchments with extensive snow cover and glaciers. The WALRUS model (Brauer et al., 2014) was developed principally for lowlands with the dominant influence of high groundwater levels. In order to provide adaptability, some models enable users to create their own structure (e.g., HEC-HMS) or to select among several methods offered for e.g., infiltration modelling, runoff and channel routing (e.g., MIKE-SHE). To obtain the optimal structure for a considered catchment, Fenicia et al. (2011) proposed a framework for model development from generic elements (reservoirs, lag functions). Similarly, the FUSE framework (Framework for Understanding Structural Errors) enables model development by combining components of various existing hydrologic models (Clark et al., 2008).

This paper presents a novel 3DNet-Catch hydrologic model developed at the Faculty of Civil Engineering of the University of Belgrade. The model is intended for simulations of the key hydrological processes in sloped catchments under a temperate climate. The 3DNet-Catch model has been developed aiming at maximising model adequacy but keeping the model structure as parsimonious as possible. The model development has principally been focused to provide (1) well-balanced structural complexity; and (2) a maximal adaptability/suitability to local conditions in a catchment, both of which are crucial issues in hydrological modelling. Specifically, well-balanced structural complexity is needed to provide realistic simulation results with modest data requirements and thereby enables model applicability even to regions with sparse observation networks. Model adaptability further enhances representation of hydrological processes in a considered catchment. Special attention during the development of 3DNet-

Catch is given to the soil routine because soil moisture dynamics is the primary source of nonlinearity in the response of this type of catchments (Todini, 1996). The soil routine of 3DNet-Catch combines simplicity of the SCS-CN method for runoff volume calculation with explicit simulation of SWC. It represents an innovative combination of the SCS method, water balance and analytically integrated nonlinear outflow equations, and the Brooks-Corey (1964) relation for unsaturated hydraulic conductivity. This approach avoids common problems in applying the SCS-CN method for continuous simulations, such as water volume conservation, runoff overestimation in-between rain events, or sudden jumps in the curve number (*CN*) values (e.g. Mishra and Singh, 2004; Cho and Engel, 2018). Another novel component of 3DNet-Catch is analytical integration of nonlinear outflow equations that describe percolation and baseflow routing. In addition, most model parameters have a physical meaning, which is an important model feature since parameter (initial) values can be inferred from soil, land use and vegetation data. The 3DNet-Catch model can be easily adapted to the conditions in a specific catchment, i.e., structure to be adjusted according to local soil and groundwater flow-related data. It also allows inclusion of various hydraulic structures, such as reservoir or diversions. The model spatial resolution can range from lumped to fully distributed. Therefore, the model can be easily adapted to fit specific application requirements, ranging from operational engineering practice to sophisticated research studies.

The focus of this paper is on a comprehensive hydrologic evaluation of the model. The proposed robust evaluation framework is intended to examine whether a hydrologic model comprising relatively simple methods for simulation of different runoff components can reasonably reproduce behaviour of catchments under a temperate climate. The evaluation framework compiles a number of methods to examine thoroughly whether the 3DNet-Catch model is: (1) comprehensively parameterised, and (2) able to reproduce reasonably a catchment hydrologic response. Model parameterisation is evaluated by conducting sensitivity, identifiability and correlation analyses. Performance metrics calculated from flows and flow-related hydrological signatures are considered to quantify model effectiveness. Further, it is assessed whether the model realistically reproduces different runoff components. For example, simulated snow cover is compared to the snow observations. Simulations of other hydrological components are assessed qualitatively, by visual inspection of the simulated series considering the presumed patterns. For the evaluation purposes, a basic, semi-lumped setup of the model is applied for simulations in the Mlava catchment in Serbia. Considerations of the model flexibility in spatial resolution or structure are beyond the scope of this paper.

2. The 3DNet-Catch Hydrologic Model

2.1. Spatial Discretisation and Catchment Computational Structure

The 3DNet-Catch model was originally developed as a component of the 3DNet Platform, which is a comprehensive GIS-oriented tool for water management. Hydroinformatic aspects of the 3DNet Platform are elaborated by Stanić et al. (2017), while this paper focuses on the 3DNet-Catch hydrologic model.

The early version of the 3DNet-Catch model was fully distributed, i.e., runoff is simulated within irregularly shaped computational units (CUs). Each unit is assigned a unique meteorological forcing and parameter set. These computational units are represented by Voronoi polygons generated over the triangles of the TIN terrain model (*Triangulated Irregular Network*) and according to the stream network and water divide. This type of discretisation provides a balance between computational accuracy and spatial resolution, i.e., simulation time (Dehotin and Braud, 2008). However, this approach is seldom applied in hydrological modelling (an example is the tRIBS model; Ivanov et al., 2004). Further model development provided spatial flexibility by enabling the CU aggregation to subcatchment or catchment level to obtain a semi-distributed or a lumped setup. Since 3DNet-Catch is implemented as Dynamic Link Library (*.dll*) it can be used independently of the 3DNet platform with externally created CUs, such as elevation zones or digitised subcatchments. Such implementation of the model also warrants computational efficiency (Stanić et al., 2017).

The model application via the 3DNet platform provides flexibility to a catchment computational structure. The catchment computational structure can easily include hydraulic structures (e.g., reservoirs, diversions). Additionally, groundwater flow can be routed to drainage point different from the topographical outlet that surface runoff is routed to.

2.2. Model Basic Description and Assumptions

Hydrological modelling with 3DNet-Catch consists of runoff volume simulation, and runoff and channel routing (Fig. 1). Runoff volume is simulated by employing three routines that represent the key hydrological processes and components: canopy interception, snow cover and soil moisture dynamics (e.g. Rakovec et al., 2016). Runoff is simulated in each CU and routed to the drainage point. Flow at a drainage point comprises direct runoff, fast groundwater (shallow aquifer) response and baseflow. All model routines are interconnected in such way that water volume conservation is preserved.

The 3DNet-Catch model is based on the following assumptions:

– No spatial heterogeneity within a computational unit: meteorological forcing, soil properties, land use and vegetation types are uniform within a CU.

– Precipitation is considered snowfall at the air temperatures below the rainfall-snowfall discrimination temperature $T_{\text{R-S}}$, and rainfall otherwise.

– Snowfall interception by canopy is not simulated. Snow refreezing, water holding capacity of the snowpack, heat exchange with the ground and temperature variation along the snowpack depth are neglected.

– Surface water retention (surface depression storage) is not simulated.

– Soil is represented by a surface and (optionally several) subsurface layers, comprising up to few meters in total. The deep groundwater system is not included in the model. Soil properties are uniform along the layer depth, but can differ across the layers.

– Water in the unsaturated soil is gravity driven and flows vertically downwards. Capillary uprise is not simulated.

– Evaporation and transpiration are modelled as distinct processes: water is assumed to evaporate from the canopy and bare surface soil, and transpires from the subsurface layer(s). The snowpack sublimation is also accounted for.

– Neither saturated nor unsaturated lateral flow among CUs is simulated; runoff is routed from a unit to the drainage point.

– No flow exchange between a watercourse and the riparian zone. Evaporation and seepage from a river section are assumed negligible.

Some of the aforementioned assumptions are generally accepted in hydrological modelling: for example, runoff is usually routed from a CU to a drainage point directly (e.g. Gupta et al., 2012), and properties of a CU are commonly considered spatially uniform (an exception is the VIC model). Snow routines of most hydrologic models are simplified: for example, a simple routine based on the degree-day method without simulating snowfall interception by canopy is also implemented in PIHM model. A sharp distinction between rainfall and snowfall is assumed in e.g. ARNO and the original version of the HBV model. Water holding capacity of the snowpack and refreezing is disregarded in many models (few exceptions are e.g. HBV, PRMS, WaSiM-ETH). Surface water retention in depressions is also frequently omitted (e.g. in ARNO and HBV), as well as capillary uprise (few exceptions to this assumption among conceptual models are e.g. HBV, WALRUS or WetSpa). Differentiation between bare soil evaporation and transpiration is made in few models, such as LISFLOOD, MIKE-SHE or tRIBS. Advanced groundwater flow simulations and channel routing cannot be performed by hydrologic models and require application of hydraulic models.

[Fig. 1. is placed here.]

2.3. Interception Routine

Rainfall interception by canopy depends on the vegetation type, and it varies throughout the growing season in deciduous vegetation. In 3DNet-Catch, vegetation is represented by a canopy reservoir with capacity $CAN(t)$ proportional to the Leaf Area Index $LAI(t)$:

$$CAN(t) = LAI(t)\frac{CAN_{\max}}{LAI_{\max}} \tag{1}$$

where $CAN_{\max}$ and $LAI_{\max}$ represent maximum values of the reservoir capacity and LAI, respectively. The $LAI(t)$ can be introduced either as an input time series or calculated for each day of the growing season according to a sine curve.

The water balance of the canopy reservoir includes rainfall $P(t)$, throughfall $R(t)$ and evaporation $E_{\text{can}}(t)$:

$$\frac{\mathrm{d}S_{\mathrm{can}}}{\mathrm{d}t} = P(t) - R(t) - E_{\mathrm{can}}(t) \quad (2)$$

where S_{can} denotes the reservoir storage (volume of water per unit area).

Canopy throughfall depends on the reservoir storage after the interception, and its current capacity:

$$R(t) = \min\left[\max\left[0; \left(S_{\mathrm{can}}(t-\Delta t) + P(t) - CAN(t)\right)\right]; P(t)\right] \quad (3)$$

where $S_{\mathrm{can}}(t\text{-}\Delta t)$ is the storage at the end of the previous time step.

Evaporation from canopy is limited by the reservoir storage and potential evapotranspiration $PET(t)$:

$$E_{\mathrm{can}}(t) = \min\left[\left(S_{\mathrm{can}}(t-\Delta t) + P(t) - R(t)\right); PET(t)\right] \quad (4)$$

2.4. Snow Routine

Snowpack water balance includes snowfall $P_{\mathrm{s}}(t)$, snowmelt $M(t)$ and sublimation $E_{\mathrm{sub}}(t)$, all of which are expressed in millimetres of water equivalent:

$$\frac{\mathrm{d}S_{\mathrm{snow}}}{\mathrm{d}t} = P_s(t) - M(t) - E_{\mathrm{sub}}(t) \quad (5)$$

where S_{snow} denotes the snowpack storage.

Sleet is not recognised in the model, so precipitation at temperatures below the threshold $T_{\mathrm{R\text{-}S}}$ is considered snowfall. Since snowfall interception by canopy is not accounted for, total snowfall is added to the snowpack (the same assumption is adopted in, e.g., the PIHM model; Qu and Duffy, 2007). Snowfall interception depends on the canopy and meteorological conditions. Consequently, its computation requires vast meteorological observations (e.g., precipitation, temperature, wind direction and velocity, relative humidity) and canopy data, such as *LAI*, canopy coverage and height (Hedstrom and Pomeroy, 1998). Coniferous vegetation can retain over 30% of snowfall (Kozii et al., 2017), but less than 5% of total snowfall is intercepted at low *LAI* values, as in deciduous vegetation during winters (Pomeroy et al., 2002). Since simulation of snowfall interception would considerably increase data requirements without substantial enhancement of simulation accuracy in catchments with prevailing deciduous vegetation in a temperate climate, considering small snowfall amount that can be intercepted during the dormant season (Pomeroy et al., 2002), this model component is omitted. However, this simplification might restrict 3DNet-Catch applicability to catchments with prevalent coniferous vegetation in cold climates.

Snowmelt $M(t)$ is computed from the air (T), snowpack (T_{snow}) and snowmelt (T_{melt}) temperatures (Neitsch et al., 2011):

$$M(t)=\min\left[\max\left[0; b_{\text{melt}}(t)\cdot snow_{\text{cov}}(t)\cdot\left(\frac{T_{\text{snow}}(t)+T(t)}{2}-T_{\text{melt}}\right)\right];\ \left(S_{\text{snow}}(t-\Delta t)+P_s(t)\right)\right] \tag{6}$$

where $b_{\text{melt}}(t)$ is the melt factor (in mm°C^{-1}day^{-1}), $snow_{\text{cov}}(t)$ represents the share of the CU area covered with snow and $S_{\text{snow}}(t\text{-}\Delta t)$ is the snowpack storage at the end of the previous time step. As snowfall occurs at temperatures above T_{melt}, it generally holds $T_{\text{R-S}}>T_{\text{melt}}$ (e.g., Schaefli et al., 2014).

The melt factor $b_{\text{melt}}(t)$ varies during the year according to a sine curve that reaches a minimum on the 21$^{\text{st}}$ December ($b_{\text{melt, 12}}$) and a maximum on the 21$^{\text{st}}$ June ($b_{\text{melt, 6}}$) (Neitsch et al., 2011):

$$b_{\text{melt}}(t)=\frac{b_{\text{melt,6}}+b_{\text{melt,12}}}{2}+\frac{b_{\text{melt,6}}-b_{\text{melt,12}}}{2}\sin\left(\frac{2\pi}{365}\left(D_n(t)-81\right)\right) \tag{7}$$

where D_{n} stands for the day of a year. To avoid model overparameterisation, dependencies of b_{melt} on e.g., elevation, wind velocity, albedo, insolation, vapour pressure, land use or aspect (Anderson, 2006; He et al., 2014) and increase during rainy days (Melloh, 1999) are neglected.

The current $snow_{\text{cov}}$ value is calculated from the snowpack storage and the minimum storage at which the entire CU area is covered with snow $S_{\text{snow,100}}$ (Neitsch et al., 2011):

$$snow_{\text{cov}}(t)=\min\left[\frac{S_{\text{snow}}(t-\Delta t)+P_s(t)}{S_{\text{snow,100}}}; 1\right] \tag{8}$$

Snowpack temperature $T_{\text{snow}}(t)$ is obtained by weighting the snowpack temperature in the previous time step $T_{\text{snow}}(t\text{-}\Delta t)$ and the current air temperature $T(t)$:

$$T_{\text{snow}}(t)=(1-\lambda)\cdot T_{\text{snow}}(t-\Delta t)+\lambda\cdot T(t) \tag{9}$$

where λ is the snowpack temperature lag factor, which takes a value between 0 and 1, and is inversely proportional to the snowpack thickness (Zhang et al., 2009).

Snowpack sublimation $E_{\text{sub}}(t)$ depends on the current snowpack storage and $PET(t)$:

$$E_{\text{sub}}(t)=\min\left[\left(S_{\text{snow}}(t-\Delta t)+P_s(t)-M(t)\right); PET(t)\right] \tag{10}$$

2.5. Soil Routine

This routine is intended for simulations of water content in the unsaturated soil zone. In 3DNet-Catch, the soil is represented by one surface layer and an arbitrary number (N_L-1) of subsurface ones. Each layer is characterised by its thickness D and following soil properties/model parameters: effective porosity p, vertical saturated hydraulic conductivity K_{sat}, volumetric water content at permanent wilting point θ_{PWP} and at field capacity θ_{FC}, and pore-size distribution index n.

Surface soil layer on the top of a soil column in 3DNet-Catch is imposed to enable differentiation between processes occurring at the soil surface and within underlying soil layer(s), such as bare soil evaporation and transpiration. This layer is considerably thinner that the subsurface ones; namely, the surface layer is few centimetres thick (e.g., Vasilić et al. (2012) assumed thickness of 10 cm), while subsurface layers can be an order of magnitude thicker.

The water balance of the surface soil layer includes throughfall and / or snowmelt P', surface runoff q_{surf}^*, percolation to the subsurface layer $w_{\mathrm{perc},1}$ and bare soil evaporation E_{soil}:

$$\frac{\mathrm{d}S_{\mathrm{surf}}}{\mathrm{d}t} = P'(t) - q_{\mathrm{surf}}^*(t) - w_{\mathrm{perc},1}(t) - E_{\mathrm{soil}}(t) \tag{11}$$

The initial surface runoff amount $q_{\mathrm{surf}}^*(t)$ is simulated employing the SCS-CN method, but it can be further augmented by excess water from the subsurface layers (saturation excess water). The SCS-CN method is selected because of its simplicity, reliable results (Mishra and Singh, 2004) and available parameter estimates due to vast field investigations (Yu, 1998):

$$q_{\mathrm{surf}}^*(t) = \begin{cases} \dfrac{\left(P'(t) - I_{\mathrm{a}}(t)\right)^2}{P'(t) - I_{\mathrm{a}}(t) + S(t)} & \text{if } P'(t) > I_{\mathrm{a}}(t) \\ 0 & \text{otherwise} \end{cases} \tag{12}$$

where I_{a} is the initial abstraction, which is obtained by subtracting canopy interception from the assumed initial abstraction $I_{\mathrm{a\_rel}}$ (dimensionless free parameter):

$$I_{\mathrm{a}}(t) = \max\left[0;\ I_{\mathrm{a\_rel}} \cdot S(t) - \left(P(t) - R(t)\right)\right] \tag{13}$$

The relation above enables continuous estimation of the initial abstraction according to the canopy and soil storages, which is important for accurate runoff simulations (Cho and Engel, 2018). The term $S(t)$ denotes the current potential soil retention capacity calculated from the SWC in the active soil zone that controls surface runoff generation and can comprise surface and subsurface layers. In this way, surface runoff is computed with respect to the actual SWC of the active zone, which is continuously simulated by applying the water balance equation, while the *CN* value is used for estimation of the maximal potential retention. A share of the L^{th} soil layer in the active zone s_{L} is calculated as follows:

$$s_{\text{L}} = \begin{cases} \min\left[1; \dfrac{S_{\text{s,max}} - \sum\limits_{L=1}^{N_{\text{L}}} D_{\text{L}} \cdot \left(p_j - \theta_{\text{PWP},j}\right)}{D_{\text{L}}}\right] & \text{if } S_{\text{s,max}} > D_1 \cdot \left(p_1 - \theta_{\text{PWP},1}\right) \\ 0 & \text{otherwise} \end{cases} \tag{14}$$

$S_{\text{s,max}}$ denotes the maximal potential retention that corresponds to the water content at permanent wilting point (antecedent moisture condition I), and it is calculated from the corresponding *CN* value (CN_1). The value of CN_1 is obtained from the *CN* that is corrected to account for actual terrain slope (see Supplementary material).

The current potential soil retention $S(t)$ is:

$$S(t) = \sum_{L=1}^{N_L+1} s_{\text{L}} \cdot \left(STO_{\text{L}} - SW_{\text{L}}(t - \Delta t)\right) \tag{15}$$

where $SW_{\text{L}}(t\text{–}\Delta t)$ is the L^{th} soil layer storage at the end of the previous time step and STO_{L} denotes capacity of the L^{th} layer calculated by multiplying its thickness by the effective porosity.

Water from a soil layer percolates under gravity into subsurface at the SWC above the residual one, which is assumed to be equal to the water content at permanent wilting point θ_{PWP}. Percolation is simulated by using an analytically integrated nonlinear outflow equation, with the Brooks-Corey relation (1964) for unsaturated hydraulic conductivity:

$$\begin{aligned} w_{\text{perc},1}(t) &= K_{\text{sat},1} \cdot \Delta t_{\text{sat}}(t) + \\ &+ \left(STO_1 - PWP_1\right) \cdot \left(S_{r,1}(t) - \left(S_{\text{r},1}^{(1-n_1)}(t) + \frac{K_{\text{sat},1}}{STO_1 - PWP_1} \cdot (n_1 - 1) \cdot \Delta t_{\text{unsat}}(t) \right)^{\frac{1}{1-n_1}} \right) \end{aligned} \tag{16}$$

where Δt_{sat} and Δt_{unsat} denote the time of percolation in saturated and unsaturated conditions, respectively (Fig. 2). The former is calculated from Eq. (17), while Δt_{unsat} is its complement to the full time step.

$$\Delta t_{\mathrm{sat}}(t)=\begin{cases}\min\left[\dfrac{SW_1^*(t)-STO_1}{K_{\mathrm{sat},1}};\ \Delta t\right] & \text{if } SW_1^*(t)\geq STO_1\\ 0 & \text{otherwise}\end{cases} \tag{17}$$

PWP_1 in Eq. (16) denotes the surface layer storage at θ_{PWP} and $S_{\mathrm{r},1}$ is effective soil saturation (Brutsaert, 2005):

$$S_{\mathrm{r},1}(t)=\min\left[\frac{SW_1^*(t)-PWP_1}{STO_1-PWP_1};\ 1\right] \tag{18}$$

where SW_1^* is the storage obtained by adding throughfall and/or snowmelt to the storage at the end of previous time step, and by subtracting initially estimated surface runoff $q_{\mathrm{surf}}{}^*$:

$$SW_1^*(t)=SW_1(t-\Delta t)+P'(t)-q_{\mathrm{surf}}^*(t) \tag{19}$$

[Fig. 2. is placed here.]

If $SW_1{}^*(t)$ exceeds the layer capacity STO_1, the storage is set to STO_1 and the excess water amount is added to the initially estimated surface runoff $q^*{}_{\mathrm{surf}}(t)$, representing saturation excess runoff:

$$SW_1^{**}(t)=\begin{cases}SW_1^*(t) & \text{if } \left(SW_1^*(t)-w_{\mathrm{perc},1}(t)\right)\leq STO_1\\ STO_1 & \text{otherwise}\end{cases} \tag{20}$$

$$q_{\mathrm{surf}}^{**}(t)=\begin{cases}q_{\mathrm{surf}}^*(t) & \text{if } \left(SW_1^*(t)-w_{\mathrm{perc},1}(t)\right)\leq STO_1\\ q_{\mathrm{surf}}^*(t)+\left(SW_1^*(t)-w_{\mathrm{perc},1}(t)-STO_1\right) & \text{otherwise}\end{cases} \tag{21}$$

Bare soil evaporation $E_{\mathrm{soil}}{}^*(t)$ is initially calculated as follows:

$$E_{\mathrm{soil}}^*(t)=\left(PET(t)-E_{\mathrm{can}}(t)-E_{\mathrm{sub}}(t)\right)\cdot \mathrm{cov}_{\mathrm{soil}}(t) \tag{22}$$

where cov_{soil} is the soil cover index representing the share of bare soil in a CU. It is calculated from the $LAI(t)$ (Supplementary material). Soil evaporation declines with soil drying, so the $E_{\mathrm{soil}}{}^*(t)$ value is corrected accordingly (Supplementary material). The surface layer storage at the end of a time step is calculated by subtracting value of the actual bare soil evaporation from $SW^{**}(t)$.

The water balance of the L^{th} subsurface soil layer comprises percolation from the overlying layer $w_{\mathrm{perc,(L-}}$

1)), percolation into the deeper layer/groundwater reservoir $w_{\mathrm{perc,L}}$ and actual transpiration, i.e., water uptake by plants $E_{\mathrm{t,L}}$ (Fig. 1):

$$\frac{\mathrm{d}S_{\mathrm{L}}}{\mathrm{d}t} = w_{\mathrm{perc,(L\text{-}1)}}(t) - w_{\mathrm{perc,L}} - E_{t,L}(t) \tag{23}$$

Percolation from the L^{th} layer is calculated using Eq. (16), but with the parameters specified for this layer. If the L^{th} layer storage after receiving percolation from the overlying layer and percolation into the deeper one/groundwater reservoir $SW_{\mathrm{L}}^{*}(t)$ exceeds its capacity, the excess water amount is added to surface runoff and the layer storage is set to STO_{L}:

$$q_{\mathrm{surf}}(t) = \begin{cases} q_{\mathrm{surf}}^{**}(t) & \text{if } SW_{\mathrm{L}}(t) \leq STO_{L} \\ q_{\mathrm{surf}}^{**}(t) + \left(SW_{\mathrm{L}}^{*}(t) - STO_{\mathrm{L}}\right) & \text{otherwise} \end{cases} \tag{24}$$

Potential transpiration ($E_{\mathrm{t,pot}}$) from the subsurface layers is calculated by subtracting actual sublimation, and actual canopy and bare soil evaporation from $PET(t)$. The $E_{\mathrm{t,pot}}$ value is distributed among the subsurface layers according to their thicknesses. Actual transpiration is calculated with respect to the current water content of these layers (Supplementary material). Storage of the L^{th} subsurface layer at the end of a time step is obtained by subtracting actual transpiration from $SW_{\mathrm{L}}^{**}(t)$, which represents smaller of $SW_{\mathrm{L}}^{*}(t)$ and STO_{L}.

The 3DNet-Catch soil routine requires estimation of numerous parameters, but the number of free parameters can be reduced by assigning the same parameter values to several/all layers. Further, the initial estimates of most parameters can be inferred from data on land-use and soil types and vegetation. To avoid overparameterisation, the basic model setup (i.e., one surface and one subsurface layer) should be used in absence of soil data that would suggest a complex structure with several different layers.

2.6. Runoff Routing

According to the basic model assumptions (Section 2.2), runoff is routed from a CU to the drainage point. This approach is frequently adopted in hydrological modelling since it is computationally efficient (Gupta et al., 2012). Surface runoff and percolation from the deepest soil layer are routed to the drainage point by applying linear and nonlinear outflow equations. Surface runoff is routed through an arbitrary number of linear reservoirs, yielding direct runoff Q_d (Fig. 3). The percolation volume inflows to a nonlinear groundwater (NLGW) reservoir with the threshold S_{max}. Water volume below S_{max} is transformed by applying the nonlinear outflow equation, resulting in baseflow Q_b. The nonlinear outflow equation is adopted to improve model performance over prolonged dry periods (Wittenberg, 1999). Water volume exceeding S_{max} is routed through a linear reservoir, and it constitutes fast groundwater discharge Q_{gw_fast}. Total flow at a drainage point is the sum of these three components:

$$Q(t)=Q_{\mathrm{d}}(t)+Q_{\mathrm{b}}(t)+Q_{\mathrm{gw\_fast}}(t) \tag{25}$$

Optionally, the integration of the 3DNet-Catch model with the 3DNet platform allows routing of fast groundwater discharge and baseflow to a different point from the surface runoff. In this way, soft data on groundwater flow, obtained from hydrogeological surveys, can be included in the model. This option is primarily intended for karstic catchments (Vasilić et al., 2012).

Each term in Eq. (25) represents mean flow rate over a time step and it is obtained by dividing the outflow volume in the time step by the time step length Δt. The outflow volumes are calculated by combining the balance and outflow equations, yielding ODEs that are analytically integrated over a computational time step (see Supplementary material). The analytical integration is preferred over numerical schemes that cause non-smoothness of the response surface, which hinder model calibration (Kavetski and Clark, 2010).

[Fig. 3. is placed here.]

The water balance of the linear reservoir for surface runoff routing consists of surface runoff from the drainage area Q_{surf} and direct runoff $Q_d(t)$:

$$\frac{\mathrm{d}S_{\mathrm{d}}(t)}{\mathrm{d}t}=Q_{\mathrm{surf}}(t)-Q_{\mathrm{d}}(t) \tag{26}$$

Surface runoff Q_{surf} is calculated assuming that surface runoff per unit area $q_{surf}(t)$ from the drainage area A is constant over a time step:

$$Q_{\mathrm{surf}}(t)=\frac{q_{\mathrm{surf}}(t)\cdot A}{\Delta t} \tag{27}$$

The reservoir coefficient K_d may be either optimised or estimated from the time of concentration

(Supplementary material). Optionally, surface runoff can be routed through several reservoirs with the same coefficient value.

Baseflow Q_b is obtained by routing of the percolation volume through the NLGW reservoir with the nonlinearity coefficient c and the threshold S_{max} (Fig. 3).

Combining the nonlinear outflow and water balance equations results in a nonhomogeneous, nonlinear first-order ODE. Assuming that the inflow to the NLGW (V_{perc}) occurs instantaneously at the beginning of a time step yields a homogenous ODE, which is further integrated over the time step following the approach presented by Todini (1996) to obtain baseflow volume V_b:

$$V_b(t) = S_{b,0} \cdot \left(1 - \left(1 - \frac{(1-c) \cdot Q_{b,0} \cdot \Delta t}{S_{b,0}}\right)^{\frac{1}{1-c}}\right) \tag{28}$$

where $S_{b,0}$ and $Q_{b,0}$ denote the reservoir storage and baseflow at the beginning of the time step, respectively. The former is the sum of the reservoir storage at the end of the previous time step and the percolation volume in the current step $V_{perc}(t)$:

$$S_{b,0} = \min\left[\left(S_b(t-\Delta t) + V_{perc}(t)\right);\ S_{max}\right] \tag{29}$$

$V_{perc}(t)$ is a product of $w_{perc}(t)$ and the baseflow drainage area A_b, which optionally may differ from the topographic drainage area A.

The threshold S_{max} is calculated from s_{max}, which represents volume per unit area and it is a free model parameter:

$$S_{max} = s_{max} \cdot A_b \tag{30}$$

Baseflow at the beginning of a time step $Q_{b,0}$ depends on the storage $S_{b,0}$:

$$Q_{b,0} = B \cdot \left(\frac{S_{b,0}}{S_{max}}\right)^c \tag{31}$$

Coefficient B denotes the highest baseflow rate and it is obtained by multiplying A_b by the maximum specific baseflow yield, i.e., baseflow rate per unit area q_d (free parameter).

Water volume exceeding S_{max} is instantaneously added to the fast groundwater reservoir with the coefficient K_{gw_fast} (Fig. 3). Optionally, this component can be disabled by imposing a high value of s_{max}.

2.7. Channel Routing

Channel routing is based on linear outflow equations, i.e., river sections are represented by linear reservoirs. This method enables peak delay and attenuation, but backwater effects cannot be simulated (Beven, 2005). The water balance of a river reach includes inflow from the upstream section and outflow at the downstream one. Other terms, such as evaporation, seepage or lateral exchange with riparian zone are neglected. Outflow volume from a reach is estimated from an analytically integrated ODE, which is obtained by combining the linear outflow and balance equations. Outflow rate is the ratio of the volume to Δt. This routine can be enhanced to include hydraulic structures and retention basins. These enhancements are presented in detail by Stanić et al. (2017).

2.8. Input Data for Simulations with 3DNet-Catch

Geo-spatial data are needed for catchment computational structure, while hydrologic simulations require hydro-meteorological data. To create catchment computational structure through the 3DNet platform, a digital terrain model (DTM) and stream network are required. Properties of the CUs necessary for simulations (area, slope and mean elevation) are automatically computed within 3DNet and forwarded to the 3DNet-Catch model. Elevation-discharge and elevation-volume curves should be provided for each reservoir in the model. If 3DNet-Catch is applied independently of the 3DNet platform, the computational structure has to be created externally using other GIS tools and all required CU properties should be supplied to the model. Data on land use, soil types and vegetative cover are not necessary for the model runs but may facilitate estimation of some model parameters.

Precipitation, maximum and mean temperatures and *PET* rates at locations of the meteorological stations are compulsory. Optionally, *PET* computation with the Hargreaves method embedded in the model requires minimum temperatures. Precipitation and temperatures can be adjusted to account for changes with elevation. Both gradients are free parameters: α represents precipitation increase (in %/100 m) and T_{lapse} is the temperature lapse rate (°C/100 m). Although precipitation gradient declines with elevation (Bardossy and Das, 2008), it is assumed constant to avoid model overparameterisation. Observed flows are necessary for model calibration. The temporal resolution of these input series should agree with computational time step.

3. Model Application

3.1. Catchment and Data

The 3DNet-Catch model is applied to the Mlava catchment upstream of Veliko Selo (Fig. 4), which is 46 km upstream of the confluence of the Mlava and Danube Rivers. The catchment covers the area of 1,277 km^2 and ranges in elevation from 100 to 1,037 m a.s.l. (mean elevation 346.9 m a.s.l.). Deciduous forests and arable cultivated land prevail, approximately 2.5 % of the catchment area is urbanised and the share of coniferous vegetation is negligible. Brown forest and acid, brown and podzolic soils are dominant soil types, while alluvial deposit and smonitza are present to a lesser extent (Fig.S2).

The Mlava River exhibits a mixed rainfall-snowmelt water regime: high flows occur from March to May due to combined rainfall and snowmelt, and the lowest flows are in September and October. High flows triggered by convective rainfall also occur during summers (June and July). The mean flow at Veliko Selo in the record period (1987-2013) amounts to 7.5 m^3/s (185.3 mm/year), with mean precipitation of 661.5 mm/year in the catchment over the same period. There are no operating reservoirs in the catchment.

Observations at the Veliko Selo stream gauge and at the three meteorological stations are used for hydrologic simulations in this paper (Fig. 4, Table 1). A stage is continuously observed at the Veliko Selo stream gauge, at which an automatic level recorder is installed. Flow rates are gauged by using either an ADCP device (Acoustic Doppler Current Profiler) or propeller-type current meters, depending on the river stage. The flow measurement campaigns are conducted several times a year to update continuously rating curves for Veliko Selo. Standard rain gauges are installed at RC Petrovac and Žagubica and daily precipitation and mean daily temperatures are observed at these stations. The Crni Vrh station is equipped with a storage rain gauge and a tipping bucket rain gauge that provides precipitation data with 10-minute temporal resolution. There are also six other gauges in the catchment at which daily precipitation and temperatures are observed; however, these observations are disregarded in this paper due to numerous gaps.

[Fig. 4. is placed here.]

[Table 1 is placed here.]

3.2. Model Setup

The model structure with one subsurface soil layer and one reservoir for surface runoff routing is employed for hydrologic simulations. Soil-related parameters are set common to both layers, except for the thickness and the saturated hydraulic conductivity. As explained in section 2.5, the surface soil layer is a few centimetres thick, while the subsurface layer thickness is significantly greater. Similarly, saturated hydraulic conductivity decreases with the soil depth (e.g., Beven, 1982). This relationship is imposed by representing subsurface layer conductivity as a common logarithm of the ratio to the surface layer conductivity (table S5). Other parameters, such as porosity and water content at field capacity and at permanent wilting point, are represented in a similar manner (table S5). Since hydraulic conductivity takes rather small values, it is presented by the common logarithm to prevent under-sampling (Marino et al., 2008). Prior parameter ranges are set for soil, land use and vegetation types inferred from local maps, and according to the related recommendations in the literature. For example, ranges of vegetation-related parameters are adopted from Breuer et al. (2003), and snow-related parameters are accepted from Anderson (2006) and Zhang et al. (2009). The *CN* prior range is inferred from land use and soil types, according to recommendations by Djorković (1984). Prior ranges of the soil-related parameters are set following Schaap et al. (2001), Ogée and Brunet (2002), Diallo and Mariko (2013) and Mathias et al. (2015). This model version comprises 25 free parameters in total, all of which are assigned a uniform prior distribution (table S5). Leaf area index *LAI* and the melt factor b_{melt} series are represented by sine curves (table S6).

The Mlava catchment is delineated into ten 100 m-wide elevation zones that are considered CUs (following Seibert and Vis, 2012). The average zone area amounts to 127.8 km^2. Model parameters are common to all zones, but the meteorological forcing is adjusted for each zone to account for change with elevation (semi-lumped model setup). Mean catchment values, estimated by applying the nearest neighbour method, are corrected following the approach presented by Panagoulia (1995):

$$\bar{P}_j = P_{\mathrm{MS}}\left(1+\frac{\alpha\cdot\left(z_j - z_{\mathrm{MS}}\right)}{100\cdot 100}\right) \tag{32}$$

$$\bar{T}_j = T_{\mathrm{MS}} + \frac{z_{\mathrm{MS}} - z_j}{100}\cdot T_{\mathrm{lapse}} \tag{33}$$

where z_{MS} denote reference altitude of the meteorological stations, z_j is mean elevation of the j^{th} zone, P_{MS} and T_{MS} are mean catchment precipitation and temperature, and $\bar{P}_j$ and $\bar{T}_j$ are mean precipitation and temperature in the zone, respectively. The precipitation gradient and lapse rate ranges are assessed from the long-term observations at the three stations (Table 1). The *PET* rates are calculated for each zone from the adjusted temperatures using the Hargreaves method (Hargreaves and Samani, 1982), with the exponent value estimated for the Western Balkans (Trajkovic, 2007):

$$PET = 0.408\cdot 0.0023\cdot\left(T+17.8\right)\cdot\left(T_{\max}-T_{\min}\right)^{0.424}\cdot R_{\mathrm{a}} \tag{34}$$

where T, $T_{\max}$ and $T_{\min}$ denote the mean, the maximum and the minimum daily temperature, respectively, and R_{a} is the extra-terrestrial radiation (in MJ m^{-2} day^{-1}). The Hargreaves method is selected because of low data requirements and reliable results in hydrological modelling (Oudin et al., 2005). The simulations are carried out with a daily time step, so daily data are used.

3.3. Hydrologic Evaluation of the 3DNet-Catch Model

A comprehensive evaluation framework is established to assess whether the 3DNet-Catch model is: (1) adequately parameterised and (2) able to reproduce catchment response. The evaluation of the basic model setup, which is presented in section 3.2, is carried out, while flexibility of the model spatial resolution, catchment computational structure and the soil routine is not considered in this paper.

The evaluation framework includes:

A. Parameterisation analysis:

   (1) Sensitivity analysis,

   (2) Parameter identifiability analysis,

   (3) Correlations among the parameters.

B. Performance analysis:

(1) Performance metrics over the calibration (1993-2003) and evaluation (2003-2013) periods,

(2) Flow-related hydrological signatures.

C. Analysis of simulated hydrological components and catchment water balance.

The model can generally be calibrated by applying an optimisation method, i.e., by coupling the 3DNet-Catch to an optimisation algorithm; however, this approach is not used here. For purpose of the model evaluation in this paper, 100,000 parameter sets are sampled from their uniform prior distributions by applying the Latin hypercube sampling. One hundred best performing sets in terms of the Kling-Gupta efficiency *KGE* (Gupta et al., 2009) in the calibration period are selected from 100,000 sampled ones. The model evaluation is based on the one hundred selected sets. All simulations are run over water years, with one preceding water year for model warm-up.

3.3.1. *Model Parameterisation Analysis*

The sensitivity analysis (SA) is conducted to detect the most influential parameters and potentially insensitive/redundant ones. The regression based SA is employed in this paper. This method relies on the multiple regression (metamodel) between the parameters and a considered model output, such as flow or a performance measure (Christiaens and Feyen, 2002). Parameter sensitivity is represented by standardised regression coefficients (SRCs), which are obtained by multiplying the regression coefficients to the ratio between standard deviations of the sampled parameters and the considered variable. High SRCs' absolute values indicate influential parameters. Metamodel validity is quantified in terms of the coefficient of determination (R^2) and variance inflation (VIF_{MAX}). The former represents goodness-of-fit, whereas the latter indicates multicollinearity among the predictors. A metamodel should be discarded in case of R^2 below 0.7 (Pan et al., 2011) and VIF_{MAX} above 10 (Christiaens and Feyen, 2002).

Parameter sensitivity of the following variables in the calibration period is analysed:

– Fluxes: flow, direct runoff and baseflow. Flow and baseflow are represented by mean values, while direct runoff is represented by its standard deviation to indicate parameters that affect runoff variability.

– Storage: SWC, canopy and snowpack storage. These variables are averaged over all elevation zones.

– Performance measures. Several performance measures calculated from daily flows are considered to identify influential parameters important for reproduction of runoff volume and dynamics. Sensitivities of *KGE* calculated for the high- and low-flow segment of the flow duration curves (FDC, Table 2) are computed to detect parameters important for reproduction of extreme flows.

Posterior distributions of well-identified parameters significantly differ from the corresponding prior (uniform) ones. The Kolmogorov-Smirnov (KS) test is applied to compare empirical cumulative posterior distribution obtained from 100 selected sets to the uniform prior for each model parameter (following Sarrazin et al., 2016). Parameter identifiability is represented by the *p*-values of the KS test statistic.

Correlations among parameters cause ridges in the response surface that hinder parameter optimisation (Schoups et al., 2010). Therefore, weak correlations suggest proper model parameterisation (Shafii and Smedt, 2009). Parameter correlations in this analysis are quantified in terms of the Spearman rank correlation coefficients.

3.3.2. *Model Performance Analysis*

The model performance is assessed from flows in the calibration (1993-2003) and evaluation (2003-2013) periods (Table 1). It is represented by *KGE* together with the ratio between the standard deviations of simulated and observed flows (*alpha*) and the correlation coefficient (*r*). Relative bias and volumetric efficiency *VE* (Criss and Winston, 2008) expose the model ability to simulate runoff volume. Equations of these performance measures, calculated from daily flows, are given in Table S7. Model ability to reproduce flow seasonality is represented by two metrics: (1) KGE_{m} calculated from monthly flows, and (2) KGE_{ia} calculated as daily values obtained by averaging flows for each particular day over the entire simulation period (following Schaefli et al., 2014). Ensemble performance is quantified in terms of *p*-factor and *r*-factor. The former denotes the percentage of observations within the 95% prediction band bounded by the 2.5^{th} and 97.5^{th} ensemble percentiles (95PPU). The latter is mean 95PPU width divided by the standard deviation of the observed flows (Sun et al., 2016). Small values of *r*-factor are preferred, while *p*-factor should tend to 1.

Additionally, model efficiency is estimated with respect to flow-related hydrological signatures. The signatures considered in this paper are selected to expose different aspects of model performance and accuracy in simulating various hydrological processes. Specifically, signatures related to FDC indicate model ability to simulate soil water redistribution and baseflow (Yilmaz et al., 2008). Therefore, performance in soil moisture dynamics is represented by *KGE* calculated from the entire FDC and its high and mid-flow segments (McMillan et al., 2017). *KGE* calculated from the low-flow FDC segment indicates the level of accuracy in the baseflow simulations. Autocorrelation and coefficient of variation expose efficiency in flow dynamics, while high and low percentiles show model ability to reproduce extreme flows. Selected signatures are briefly outlined in Table 2 and further detail can be found in the literature (Yilmaz et al., 2008; Westerberg and McMillan, 2015; Westerberg et al., 2016).

[Table 2 is placed here.]

3.3.3. *Hydrological Components and Water Balance of the Catchment*

This part of the evaluation framework implies analysis of individual hydrological components. To this end, observations of various hydrologic variables such as snow cover, soil moisture or groundwater should be considered (e.g. Rakovec et al., 2016). In the Mlava catchment, only data on snow cover are available. However, assessment of snow simulation accuracy is rather challenging in this catchment, since snowpack thickness observations at the Žagubica station (1993-2000) are only available. These observations are compared to the simulated snow water equivalent in the third elevation zone, since Žagubica is located within this zone. Agreement between these series is represented by Spearman rank correlation coefficients. In this analysis, it is assumed that the higher snowpack thickness implies higher total water content. Agreement between simulated and observed snowpack represents an effective model evaluation measure, considering that snowpack observations are not used to constrain model parameters in this case study. Efficiency in flow simulations during the snow season (January through April) is also an indicator of snow simulation accuracy.

Additionally, key simulated variables are inspected visually considering the expected patterns. Although such a comparison provides a mere qualitative model evaluation, it is very important as it indicates whether the model provides "right answers for the right reasons" (Kirchner, 2006). The following simulated variables are presented: flow, direct runoff and baseflow at Veliko Selo. Furthermore, SWC, canopy and snowpack storage and actual *ET* (*AET*) within the third elevation zone are also shown. This particular zone is selected since its mean elevation corresponds to the mean catchment elevation.

4. RESULTS AND DISCUSSION

4.1. The Evaluation Results: Model Parameterisation

Parameter sensitivity (SA), identifiability and correlations among the parameters are analysed to evaluate the effectiveness of 3DNet-Catch parameterisation. The first step of the SA is the metamodels' validity assessment. Most regression metamodels yield coefficients of determination (R^2) between 0.72 (*KGE* of the low-flow FDC segment) and 0.99 (canopy storage). However, four metamodels resulted in somewhat lower R^2: the Nash-Sutcliffe efficiency *NSE* (0.60), bias and total flows (0.64), and *KGE* of the high-flow FDC segment (0.66). Since these R^2 are only slightly below the recommended threshold of 0.7, these metamodels are accepted as valid and retained in the SA. Bias and *NSE* yield the highest R^2 out of several considered performance measures, and, therefore, are selected to identify parameters important for reproducing runoff volume and dynamics (Krause et al., 2005). The maximum VIF amounts to 3.1 (*NSE*), indicating valid metamodels.

The absolute SRC values are presented in Fig. 5. Fig. 5A shows parameter sensitivity of flows, direct runoff and baseflow. Flow is largely influenced by the precipitation gradient α, parameters of the soil routine (porosity, the thickness of the subsurface layer, pore size distribution index, saturated conductivities) and $LAI_{\max}$. The precipitation gradient affects total precipitation and consequently runoff volume. High sensitivity to α variations suggests the significance of precipitation data, while sensitivity to the soil-related parameters indicates the importance of soil moisture dynamics for flow simulations. Direct runoff is mainly influenced by the soil conductivities and the reservoir coefficient, K_d (in control of surface to direct runoff transformation), while sensitivity to α is lower than in flows. Mean baseflow is sensitive to the hydraulic conductivities, as well as percolation to the NLGW reservoir (not shown here). Low sensitivity to the baseflow-related parameters suggests that baseflow rates are governed by percolation from the unsaturated soil rather than its routing. To analyse the impact of maximum baseflow yield q_d and coefficient c on baseflow dynamics, a temporal SA is conducted with a daily time step (following Sieber and Uhlenbrook, 2005). The SRC values of these parameters are generally low (Fig. S4), but clearly correlated to baseflow rates. For example, the sensitivity to parameter c variations increases during prolonged dry periods, i.e., it becomes "more active" during these periods thereby implying plausible parameterisation (Pfannerstill et al., 2015). Additionally, parameter q_d is engaged in the analytical integration of the nonlinear outflow equation, and facilitates model calibration. Fast groundwater discharge is not considered here since the corresponding metamodel yields low R^2.

Fig. 5B presents parameter sensitivity of three types of storage. Soil water content is influenced by the porosity and subsurface layer thickness (their product comprises almost total soil capacity). Canopy storage is primarily affected by CAN_{max}. Snowpack storage is sensitive to $T_{\mathrm{R\text{-}S}}$ and T_{melt}, with lower sensitivity to other snow-related parameters. Temporal SA to these snow-related parameters reveals an increased sensitivity to $S_{\mathrm{snow,100}}$ and λ during snow ablation periods (Fig. S5). The sensitivity of the snowpack storage to the melt factors is low, especially to $b_{\mathrm{melt,12}}$, suggesting that snowmelt simulated with a daily time step is influenced mainly by the air temperature and the available snow storage in the Mlava catchment. Seasonality in b_{melt} is not pronounced, possibly due to a relatively short snow season in this catchment; hence, the $b_{\mathrm{melt}}(t)$ could be represented by a constant value.

The accuracy of flow volume simulation results is mainly affected by α, some soil-related parameters and LAI_{max}. The model ability to reproduce runoff dynamics is influenced by the hydraulic conductivities and the reservoir coefficient K_d, all of which affect direct runoff. The precipitation gradient, K_d and the most soil-related parameters are important for high-flow simulations. Model performance in low-flows is sensitive to the threshold S_{max}, and to a lesser extent to a subset of soil-related parameters.

[Fig. 5. is placed here.]

The results indicate insensitivity to CN and initial abstraction $I_{\mathrm{a\_rel}}$, so a temporal SA with respect to these parameters is conducted (Fig. 6). Increased SRCs are identified during rain events, which is consistent with their role in surface runoff simulations since these parameters define partitioning between infiltration and excess precipitation. These results suggest the importance of those parameters for surface runoff simulations, and consequently flows and model efficiency.

[Fig. 6. is placed here.]

Fig. 7 shows one hundred best parameter realisations relative to their prior ranges. Empirical posterior distributions of these sets are compared to the corresponding prior uniform distributions using the KS test. Parameters that result in the KS test null hypothesis rejection at the 5% significance level are considered to be well-identified (i.e., statistically significant, denoted by green circles in Fig. 7A). The parameters yielding the hypothesis rejection at 25% significance level (i.e., potentially significant, denoted by yellow triangles in Fig. 7A) are also considered well-identified (Plavsic et al., 2016). Most parameters for this application of the 3DNet-Catch model are well-identified. Few parameters, such as $CAN_{\max}$, the melt factors, few soil- and baseflow-related parameters are not properly identified (*p*-values exceed 25%, red diamonds in Fig. 7A). Since low identifiability might be attributed to the performance measure used for parameter selection, the KS test is repeated with 100 best performing sets according to *KGE* calculated from log-transformed flows ($KGE_{\log Q}$). These results (Fig. 7B) show that $I_{\mathrm{a\_rel}}$, θ_{FC}, *n* and baseflow-related parameters are well-identified. Regardless of the performance measure, few parameters exhibit low identifiability: $CAN_{\max}$, T_{melt}, the melt factors and θ_{PWP}. Low identifiability of these parameters could be explained by the fact that they presented as functions of other parameters (Table S5), which should be avoided if possible. Parameter identifiability could also be discussed considering the width of the prior ranges. In this study, the prior ranges are set quite narrow (including $CAN_{\max}$, T_{melt} and θ_{PWP}), and wider prior ranges could result in lower *p*-values of the KS test. This assumption, however, should be tested in further research.

The matrix of Spearman rank correlation among the selected parameters is shown in Fig. 8. The median value of the correlation coefficients amounts to -0.01, with 2.5$^{\mathrm{th}}$ and 97.5$^{\mathrm{th}}$ percentiles of -0.25 and 0.23, respectively. As none of the coefficients exceeds 0.6 (the largest coefficient is 0.58), the parameters are considered uncorrelated (Blasone et al., 2007).

Altogether, results of the sensitivity, identifiability and correlation analyses in this case study suggest that 3DNet-Catch is adequately parameterised notwithstanding the large number of parameters. Most parameters affect the simulated variables and/or model performance, which is evident either over the entire simulation period or sporadically. They are also well identifiable and uncorrelated. The snow routine might be simplified by neglecting the melt factor seasonality (for this catchment).

[Fig. 7. is placed here.]

[Fig. 8. is placed here.]

4.2. The Evaluation Results: Model Performance

Performance of 100 selected parameter sets in the calibration and evaluation periods is shown in Fig. 9. The ensemble performance is represented by the Kling-Gupta efficiency coefficients calculated from daily (*KGE*) and monthly flows (KGE_{m}), and from daily flows averaged for a particular day over the entire simulation period (KGE_{ia}). Additionally, the ratio between standard deviations of the observed and simulated flows (alpha) and their correlation coefficient (*r*), volumetric efficiency (*VE*) and bias are shown. To provide a frame of reference, these performance measures are compared to those obtained of the HBV-light model (Seibert and Vis, 2012) ensemble, presented by Todorović and Plavšić (2015). Median *KGE* in both periods amounts to 0.67, indicating satisfactory performance of 3DNet-Catch (Pechlivanidis et al., 2014). The HBV-light ensemble resulted in the median *KGE* of 0.55 and 0.68 in the calibration and evaluation periods, respectively. Since the models are forced with observations from only three meteorological stations in the catchment, improved input data quality (i.e., wide observation network coverage) may well yield higher efficiency. Sensitivity of efficiency to input data quality, however, requires model application to catchments with an extensive observation network coverage. Furthermore, some ensemble members perform better in the evaluation period, which corroborates the results obtained by Todorović and Plavšić (2015). Such results could be attributed to generally higher flows in the evaluation period (Table 1), since increased accuracy in higher flow rates can be expected with the performance measure used for parameter selection (Pechlivanidis et al., 2014). However, the 3DNet-Catch ensemble of one hundred best performing sets selected according to $KGE_{\log Q}$ behaves in a similar manner, i.e., it yields the median *KGE* values of 0.50 and 0.65 over the calibration and evaluation periods, respectively (not shown here). These results might indicate higher data quality in the evaluation period. The correlation coefficient values are satisfactory (Moriasi et al., 2007), and exceed those obtained by the HBV-light model (0.65 and 0.75 in the calibration and evaluation, respectively).

However, the standard deviation is slightly overestimated in the evaluation period by the 3DNet-Catch model, as opposed to the HBV-light ensemble. The values of KGE_m and KGE_{ia}, and monthly flows at Veliko Selo, which are generally contained within the 95PPU during both periods (Fig. 10), suggest that the model accurately reproduces flow seasonality. The monthly flows are overestimated during the late summers and autumns by the 95PPU, and slightly underestimated in early spring (combination of rainfall and snowmelt). Similar results were obtained with the HBV-light model, which overestimated flows from April through August. The bias values obtained with 3DNet-Catch are rather low: the median value amounts to -1.8% for the calibration, and 6.5% for the evaluation period, demonstrating model ability to reproduce runoff volume. The HBV-light model resulted in the bias values of 12.8% and 2.7%, and the median *VE* values of 0.87 and 0.94 over the calibration and evaluation, respectively. Ensemble performance is represented by *p*-factor, which amounts to 0.76 and 0.77 in the calibration and evaluation periods, respectively, and by *r*-factor of 0.77 in both periods. These results denote relatively narrow 95PPU that encompasses a large percentage of the observed flows. The 3DNet-Catch ensemble is slightly wider than the HBV-light ensemble, but encompasses higher per cent of the observed flows: HBV-light resulted in the *p*-factor values of 0.6 and 0.65, and *r*-factor of 0.69 and 0.75 during the calibration and evaluation periods, respectively.

[Fig. 9. is placed here.]

[Fig. 10. is placed here.]

The evaluation of the model performance also involves hydrologic signatures (Table 3). Comparison of mean flows confirms model ability to reproduce runoff volume. The coefficients of variation indicate overestimated flow variance in the evaluation period. One-day autocorrelation is marginally overestimated: for example, simulated low flows are aligned along recession curves, as opposed to the noisy observations. High values of KGE_{FDC} suggest that the entire FDC is well reproduced by the ensemble (supported by high *p*-factors in both periods, Fig. 11). *KGE*s of the FDC segments further reflect performance in high-, mid- and low-flows. Performance in the high-flow FDC segment (0-0.05 exceedance probability) is good, especially during the evaluation period. FDCs in Fig. 11 show that the observations are contained within the ensemble range during the evaluation period, but underestimated during the calibration. The 3DNet-Catch model properly reproduces the mid-flow FDC segment; however, there is a considerable dispersion across the ensemble (indicated by low 2.5th percentile of KGE_{MF}). Performance of the 3DNet-Catch model in low flows is somewhat lower than in other FDC segments, although some ensemble members reproduce this FDC segment well (indicated by high 97.5th percentile of KGE_{LF}). Extreme flow percentiles in Table 3 are generally within 95PPU bounds: high percentiles of the observed and simulated flows are comparable, although extreme low flows are underestimated by most ensemble members.

[Table 3 is placed here.]

[Fig. 11. is placed here.]

4.3. The Evaluation Results: Hydrological Components and Water Balance of the Catchment

Simulated hydrological components are analysed to assess whether their dynamics corresponds to expected patterns. Fig. 12 presents simulated variables by the best performing parameter set in the evaluation period with *KGE* and bias of 0.77 and 7.5%, respectively. A good agreement between simulated and observed flows is apparent: simulated hydrograph corresponds to the observed one in terms of rising and recession limbs, and in peak timings. The log-transformed hydrographs further illustrate the agreement in hydrograph recession limbs and low flows in general. Surface and direct runoff values are generated occasionally, after rain events or snowmelt, while the increase in baseflow is delayed. Direct runoff is considerably larger than baseflow, resulting in overall flow variability. Baseflow rates in Fig. 12 do not exceed 3 m^3/s, and are consistent with the long-term average flows at Veliko Selo during dry periods (Prohaska et al., 2009). Fast groundwater response is not generated due to high s_{max} value of this particular set. Runoff coefficient estimated from the simulated flows amount to 0.34, which is equal to the long-term estimate for this catchment made by Prohaska et al. (2009).

Percolation rates correlate well with SWC, with the highest values during winters and early springs. Percolation rates are almost two order of magnitude smaller than surface runoff rates, which corresponds to the ratio between direct runoff and baseflow. Canopy storage is up to 2.5 mm (CAN_{max} is 5.7 mm), which is a reasonable estimate for deciduous vegetation in a temperate climate (Breuer et al., 2003). The Spearman rank correlation coefficient, which is calculated between observed snowpack thickness at Žagubica and simulated snow storage, is 0.71 (1993-2000). The *AET* values (e.g., 502 mm/year in the evaluation period) are consistent the with the long-term water balance that suggests 473 mm/year (Prohaska et al., 2009). Since the simulated hydrological components strongly concur with the expected patterns in the Mlava catchment, indicating realistic representation of processes in the 3DNet-Catch model.

[Fig. 12. is placed here.]

4.4. Summary of the Results of the 3DNet-Catch Model Evaluation

The model evaluation suggests that the 3DNet-Catch model accurately reproduces runoff volume and FDCs although it is forced with observations from a sparse observation network. Bias in runoff volume in both simulation periods is below the margin of error considering rating curve uncertainties (Di Baldassarre and Montanari, 2009). Values of *KGE* and 1-day AC signature indicate that runoff dynamics is satisfactorily reproduced. Most importantly, model efficiency in both periods is broadly similar, demonstrating its transferability.

High performance is obtained in the mid- and high-flow FDC segments, which can be attributed to accuracy in soil moisture simulations (Yilmaz et al., 2008). High efficiency together with the high sensitivity to the soil-related parameters indicates plausible parameterisation of the soil routine. Additionally, simulated SWC values correspond to the expected pattern in a catchment located in a temperate climate (high content in early springs and low in late summers). Adaptability to local conditions and physically meaningful parameters represent additional advantages of this routine.

Good model performance in high flows and runoff dynamics also depends on runoff routing accuracy. Satisfactory performance, high SRC and identifiability of the linear reservoir coefficient K_d indicate a proper parametrisation of this routing component. These results also suggest that the spatial lumping of runoff routing yields reliable results with a daily computational step.

Variability of low-flow performance across the ensemble suggests that parameters are not sufficiently conditioned with respect to this flow component in these analyses, rather than model structure inadequacies. The use of performance measures that put emphasis on low flows (e.g., logarithmic or square root transformations, Oudin et al., 2006) could potentially improve efficiency in this regard. To test this assumption, additional simulations are carried out with 100 best parameter sets selected according to $KGE_{\mathrm{log}Q}$. These sets resulted in higher KGE_{LF} values than those in Table 3: namely, the 2.5$^{\mathrm{th}}$, 50$^{\mathrm{th}}$ and 97.5$^{\mathrm{th}}$ percentiles amount to 0.11, 0.46 and 0.81, respectively. Furthermore, observed monthly flows in June through December are within the 95PPU, except for November flows, which is still slightly overestimated (not shown here). Therefore, model performance in low-flows requires further research aimed at identifying a proper calibration strategy. Underestimation of extremely low flows is related to the accuracy of low-flow observations: namely, observed flows over prolonged dry periods take constant values, while simulated recessions lead to flow decrease in time.

High flows in this catchment are often triggered by snowmelt, thus model performance in high-flows is also conditioned on the accuracy of snow simulations. The model satisfactorily reproduces high flows, although many ensemble members underestimated early spring flows (caused by combined rain events and snowmelt). These results, along with low sensitivity and identifiability of some snow-related parameters reveal a scope for improvement of this routine. Enclosure of the snowpack observations in the calibration procedure should be considered as well.

A visual inspection of hydrographs reveals that some rainfall events during summers and autumns are not accompanied by an increase in the observed hydrographs, as opposed to the simulated flows. These discrepancies can be attributed to the spatial rainfall representation in this modelling setup and sparse raingauge network that cannot capture the spatial heterogeneity of summer convective rainfall events. A fully distributed setup and finer spatial resolution of rainfall observations could potentially improve simulation accuracy during these events, as well as the overall model performance.

Although the evaluation results suggest proper parameterisation of 3DNet-Catch, it should be noted that the evaluation presented in this paper is based on a single catchment. The model application in other catchments with different hydrologic regime, as well as model comparison to the other models, requires further research.

5. CONCLUSIONS AND FUTURE RESEARCH

The 3DNet-Catch hydrologic model and a comprehensive evaluation of the basic model setup are presented in this paper. The model is conceived as a trade-off between oversimplified, parsimonious models and demanding, complex ones, enabling plausible simulation results with modest data and computational requirements. The central point of the model is its soil routine, which combines the SCS-CN method for estimation of maximum soil retention, the nonlinear outflow equation and the Brooks-Corey relation for unsaturated hydraulic conductivity. This routine can be adapted according to soil data, which is a distinct feature of 3DNet-Catch. The soil routine and runoff routing include analytically integrated nonlinear outflow equations, thereby preventing issues caused by the application of numerical methods.

To assess parametrisation and performance of 3DNet-Catch, a comprehensive evaluation framework is established and used with a semi-lumped model setup of the Mlava catchment. The evaluation results suggest the following:

- The basic structure of 3DNet-Catch (i.e., semi-lumped model setup, structure with one surface and one subsurface soil layer, and surface routing through a single linear reservoir) provides satisfactory, reasonable simulation results even with forcing from a sparse observation network.
- The soil routine parametrisation results in a good representation of soil water dynamics, and consequently in good model performance for mid- and high-range flows. The use of physically meaningful parameters represents an appealing feature of this routine.
- A simple degree-day based method provides realistic simulation results for the snowpack and flows during melt seasons, although there is a scope for improvement. The results obtained in the Mlava catchment suggest that seasonality in the melt factor can be neglected.
- The linear outflow equation for surface runoff routing enables proper reproduction of high flows in terms of both flow rates and peak timing.
- A nonlinear groundwater reservoir with a threshold enables a reasonable representation of groundwater response, but the estimation of the baseflow-related parameters requires performance measures that emphasise this flow component.

The presented features and evaluation results suggest that the 3DNet-Cacth model is suitable for runoff simulations in mesoscale sloped catchments under a temperate climate. Good performance with modest data requirements enables 3DNet-Catch applicability in operational practice. Specifically, it can be used for addressing various issues related to water resources management. For example, values of most model parameters can generally be inferred from soil, land use and vegetation data. Stanić et al. (2017) relied on this model feature to reconstruct an extreme flood in Serbia in May 2014, since a conventional model calibration could have not be performed due to pronounced uncertainties in the observed flows. This model was used afterwards by the water authorities for evaluation of various flood mitigation measures (Babić Mladenović and Divac, 2015). The 3DNet-Catch model includes the SCS-CN method, thus it can be readily applied for e.g. assessment of various scenarios of land use change, particularly if a distributed setup is employed. Being implemented as a Dynamical Link Library (*.dll*), the model is computationally efficient, and thus particularly convenient for climate change impact studies that are usually computationally intensive. Realistic simulation results across different flow ranges pose an additional model advantage in such applications. In addition, flexibility in model structure or spatial resolution makes it a particularly appealing tool for hydrologic research studies.

For future considerations, the snow routine can be enhanced by introducing a smooth transition between snowfall and rainfall, or an increase in the melt factor during rain-on-snow events. The model performance during snow melt season could be improved by including snow cover data into the model calibration. The enclosure of groundwater-surface interactions (capillary rise) in the model might enhance model performance in catchments with high groundwater table. The first-order explicit Euler method implemented in the routines for runoff volume simulations can be replaced by a more robust explicit numerical method (e.g., the Runge-Kutta scheme). Furthermore, storage-dependant flow exchange among CUs rather than routing to a catchment outlet can be implemented. The channel routing component can be improved by either embedding robust routing methods, or by coupling to a hydraulic model, as suggested by Stanić et al. (2017). The 3DNet-Catch model can also be coupled with a groundwater model, such as UGROW (Pokrajac and Stanić, 2010). An integration of 3DNet-Catch with other models and the storage-dependant runoff routing is generally not intended for the engineering practice due to increased computational demands, but this would be a promising avenue of research.

ACKNOWLEDGEMENT

The research presented in this paper is supported by the Ministry of Education, Science and Technological Development of the Republic of Serbia (projects TR37005 and TR37010). Data used are provided by the Republic Hydrometeorological Service of Serbia. We express our deepest gratitude to prof. Dragan Savić from the University of Exeter, for the constructive suggestions and valuable help with the manuscript preparation. We are grateful to prof. Zorana Naunović from the University of Belgrade, for proof reading the manuscript. We would like to thank to dr Eylon Shamir from the Hydrologic Research Center, prof. Slobodan Djordjević from the University of Exeter, dr Massimiliano Zappa from Swiss Federal Research Institute WSL, and an anonymous reviewer for their constructive suggestions that helped us to improve the manuscript.

Declaration of Interests

None.

REFERENCES

Anderson, E., 2006. Snow Accumulation and Ablation Model – SNOW-17.

Babić Mladenović, M., Divac, D. (Eds.), 2015. Studija unapredjenja zaštite od voda u slivu reke Kolubare (Improvement of Flood Control in the Kolubara River Basin). “Jaroslav Cerni” Institute for the Development of Water Resources.

Bardossy, A., Das, T., 2008. Influence of rainfall observation network on model calibration and application. Hydrol. Earth Syst. Sci. 12, 77–89.

Bergström, S., Frosman, A., 1973. Development of a conceptual deterministic rainfall-runoff model. Nord. Hydrol. 4, 147–170.

Beven, K., 2001a. Rainfall-Runoff Modelling - The Primer. John Wiley & Sons, West Sussex.

Beven, K., 2001b. How far can we go in distributed hydrological modelling ? Hydrol. Earth Syst. Sci. 5, 1–12.

Beven, K., 1982. On subsurface storm flow: an analysis of response times. Hydrol. Sci. - J. des Sci. Hydrol. 4, 505–521.

Beven, K., Binly, A., 1992. The Future of Distributed Models: Model Calibration and Uncertainty Prediction. Hydrol. Process. 6, 279–298.

Beven, K.J., 2005. Rainfall-runoff Modeling: Introduction, in: Anderson, M., McDonnell, J. (Eds.), Encyclopedia of Hydrological Sciences. John Wiley & Sons Ltd.

Blasone, R.-S., Madsen, H., Rosbjerg, D., 2007. Parameter estimation in distributed hydrological modelling: comparison of global and local optimisation techniques. Nord. Hydrol. 38, 451. doi:10.2166/nh.2007.024

Boyle, D.P., Gupta, H. V., Sorooshian, S., Koren, V., Zhang, Z., Smith, M., 2001. Toward improved streamflow forecasts: Value of semidistributed modeling. Water Resour. Res. 37, 2749–2759. doi:10.1029/2000WR000207

Brauer, C.C., Teuling, A.J., Torfs, P.J.J.F., Uijlenhoet, R., 2014. The Wageningen Lowland Runoff Simulator (WALRUS): a lumped rainfall–runoff model for catchments with shallow groundwater. Geosci. Model Dev. 7, 2313–2332. doi:10.5194/gmd-7-2313-2014

Breuer, L., Eckhardt, K., Frede, H.-G., 2003. Plant parameter values for models in temperate climates. Ecol. Modell. 169, 237–293. doi:10.1016/S0304-3800(03)00274-6

Brooks, R., Corey, A., 1964. Hydraulic properties of porous media, Hydrology Papers, Colorado State University. Colorado State University, Fort Collins.

Brutsaert, W., 2005. Hydrology: An Introduction, 1st ed. Cambridge University Press, Cambridge, UK.

Chang, C.L., Chao, Y.C., 2014. Effects of spatial data resolution on runoff predictions by the BASINS model. Int. J. Environ. Sci. Technol. 11, 1563–1570. doi:10.1007/s13762-013-0342-9

Chiew, F.H.S., Kirono, D.G.C., Kent, D.M., Frost, A.J., Charles, S.P., Timbal, B., Nguyen, K.C., Fu, G., 2010. Comparison of runoff modelled using rainfall from different downscaling methods for historical and future climates. J. Hydrol. 387, 10–23. doi:10.1016/j.jhydrol.2010.03.025

Cho, Y., Engel, B.A., 2018. Spatially distributed long-term hydrologic simulation using a continuous SCS CN method-based hybrid hydrologic model. Hydrol. Process. 32, 904–922. doi:10.1002/hyp.11463

Christiaens, K., Feyen, J., 2002. Use of sensitivity and uncertainty measures in distributed hydrological modeling with an application to the MIKE SHE model. Water Resour. Res. 38, WR000478, 8-1-8-15. doi:10.1029/2001WR000478

Ciarapica, L., Todini, E., 2002. TOPKAPI: A model for the representation of the rainfall-runoff process at different scales. Hydrol. Process. 16, 207–229. doi:10.1002/hyp.342

Clark, M.P., Slater, A.G., Rupp, D.E., Woods, R.A., Vrugt, J.A., Gupta, H. V., Wagener, T., Hay, L.E., 2008. Framework for Understanding Structural Errors (FUSE): A modular framework to diagnose differences between hydrological models. Water Resour. Res. 44, W0B02, 1-14. doi:10.1029/2007WR006735

Criss, R.E., Winston, W.E., 2008. Do Nash values have value? Discussion and alternate proposals. Hydrol. Process. 22, 2723–2725. doi:10.1002/hyp

Dehotin, J., Braud, I., 2008. Which spatial discretization for distributed hydrological models? Proposition of a methodology and illustration for medium to large-scale catchments. Hydrol. Earth Syst. Sci. 12, 769–796. doi:10.5194/hess-12-769-2008

Diallo, D., Mariko, A., 2013. Field capacity (FC) and permanent wilting point (PWP) of clay soils developed on Quaternary alluvium in Niger River loop (Mali). Int. J. Eng. Res. Appl. 3, 1085–1089.

Di Baldassarre, G., Montanari, A., 2009. Uncertainty in river discharge observations: a quantitative analysis. Hydrol. Earth Syst. Sci. 13, 913–921. doi:10.5194/hess-13-913-2009

Djorković, M., 1984. Odredjivanje hidrološke grupe zemljišta pri definisanju oticanja u metodi SCS. (Assessment of hydrological soil type for runoff modelling with the SCS method) Vodoprivreda 87, 57–60.

Ebel, B.A., Loague, K., 2006. Physics-based hydrologic-response simulation: Seeing through the fog of equifinality. Hydrol. Process. 20, 2887–2900. doi:10.1002/hyp.6388

Feldman, A., 2000. Hydrologic Modeling System HEC-HMS - Technical Reference Manual.

Fenicia, F., Kavetski, D., Savenije, H.H.G., 2011. Elements of a flexible approach for conceptual hydrological modeling: 1. Motivation and theoretical development. Water Resour. Res. 47, 1–13. doi:10.1029/2010WR010174

Fenicia, F., Savenije, H.H.G., Matgen, P., Pfister, L., 2008. Understanding catchment behavior through stepwise model concept improvement. Water Resour. Res. 44, W01402, 1–13. doi:10.1029/2006WR005563

Gupta, H. V., Kling, H., Yilmaz, K.K., Martinez, G.F., 2009. Decomposition of the mean squared error and NSE performance criteria: Implications for improving hydrological modelling. J. Hydrol. 377, 80–91. doi:10.1016/j.jhydrol.2009.08.003

Gupta, H. V, Clark, M.P., Vrugt, J.A., Abramowitz, G., Ye, M., 2012. Towards a comprehensive assessment of model structural adequacy. Water Resour. Res. 48, W08301, 1–16. doi:10.1029/2011WR011044

Hargreaves, G.H., Samani, Z.A., 1982. Estimating Potential Evapotranspiration. J. Irrig. Drain. Eng. 108, 225–230.

He, Z.H., Parajka, J., Tian, F.Q., Blöschl, G., 2014. Estimating degree-day factors from MODIS for snowmelt runoff modeling. Hydrol. Earth Syst. Sci. 18, 4773–4789. doi:10.5194/hess-18-4773-2014

Hedstrom, N.R., Pomeroy, J.W., 1998. Measurements and modelling of snow interception in the boreal forest. Hydrol. Process. 12, 1611–1625. doi:10.1002/(SICI)1099-1085(199808/09)12:10/11<1611::AID-HYP684>3.0.CO;2-4

Hrachowitz, M., Clark, M., 2017. HESS Opinions: The complementary merits of top-down and bottom-up modelling philosophies in hydrology. Hydrol. Earth Syst. Sci. Discuss. 21, 1–22. doi:10.5194/hess-2017-36

Ivanov, V.Y., Vivoni, E.R., Bras, R.L., Entekhabi, D., 2004. Catchment hydrologic response with a fully distributed triangulated irregular network model. Water Resour. Res. 40, W11102, 1–23. doi:10.1029/2004WR003218

Jakeman, A.J., Hornberger, G.M., 1993. How much complexity is warranted in a rainfall-runoff model? Water Resour. Res. 29, 2637–2649. doi:10.1029/93WR00877

Kauffeldt, A., Wetterhall, F., Pappenberger, F., Salamon, P., Thielen, J., 2016. Environmental Modelling & Software Technical review of large-scale hydrological models for implementation in operational flood forecasting schemes on continental level. Environ. Model. Softw. 75, 68–76. doi:10.1016/j.envsoft.2015.09.009

Kavetski, D., Clark, M.P., 2010. Ancient numerical daemons of conceptual hydrological modeling: 2. Impact of time stepping schemes on model analysis and prediction. Water Resour. Res. 46, W10511, 1–27. doi:10.1029/2009WR008896

Kirchner, J.W., 2006. Getting the right answers for the right reasons: Linking measurements, analyses, and models to advance the science of hydrology. Water Resour. Res. 42, W03S04, 1-5. doi:10.1029/2005WR004362

Krause, P., Boyle, D.P., Base, F., 2005. Comparison of different efficiency criteria for hydrological model assessment. Adv. Geosci. 5, 89–97.

Kuczera, G., Parent, E., 1998. Monte Carlo assessment of parameter uncertainty in conceptual catchment models: the Metropolis algorithm. J. Hydrol. 211, 69–85. doi:10.1016/S0022-1694(98)00198-X

Liang, X., Lettenmaier, D.P., Wood, E.F., Burges, S.J., 1994. A simple hydrologically based model of land surface water and energy fluxes for general circulation models. J. Geophys. Res. 99, 14415–14428. doi:10.1029/94JD00483

Lindström, G., Johansson, B., Persson, M., Gardelin, M., Bergstrm, S., 1997. Development and test of the distributed HBV-96 hydrological model. J. Hydrol. 201, 272–288.

Lindström, G., Pers, C.P., Rosberg, R., Strömqvist, J., Arheimer, B., 2010. Development and test of the HYPE (Hydrological Predictions for the Environment) model – A water quality model for different spatial scales. Hydrol. Res. 41, 295–319.

Marino, S., Hogue, I.B., Ray, C.J., Kirschner, D.E., 2008. A methodology for performing global uncertainty and sensitivity analysis in systems biology. J. Theor. Biol. 254, 178–196. doi:10.1016/j.jtbi.2008.04.011

Markstrom, S.L., Regan, R.S., Hay, L.E., Viger, R.J., Webb, R.M.T., Payn, R.A., LaFontaine, J.H., 2015. PRMS-

IV, the Precipitation-Runoff Modeling System, Version 4, in: U.S. Geological Survey Techniques and Methods, Book 6, Chapter 7 of Section B, Surface Water. U.S. Geological Survey, Reston, Virginia.

Mathias, S.A., Skaggs, T.H., Quinn, S.A., Egan, S.N.C., Finch, L.E., Oldham, C.D., 2015. A soil moisture accounting-procedure with a Richards' equation-based soil texture-dependent parameterization. Water Resour. Res. 51, 506–523. doi:10.1016/0022-1694(68)90080-2

McMillan, H., Westerberg, I., Branger, F., 2017. Five guidelines for selecting hydrological signatures. Hydrol. Process. 31, 4757–4761. doi:10.1002/hyp.11300

Melloh, R.A., 1999. A Synopsis and Comparison of Selected Snowmelt Algorithms. Hanover, New Hampshire.

Mendoza, P.A., Clark, P.M., Barlage, M., Rajagopalan, B., Samaniego, L., Abramowitz, G., Gupta, H., 2014. Are we unnecessarily constraining the agility of complex process-based models? Water Resour. Res. 51, 1–13. doi:10.1002/2014WR015820.Received

Mishra, S.K., Singh, V.P., 2004. Long-term hydrological simulation based on the Soil Conservation Service curve number. Hydrol. Process. 18, 1291–1313. doi:10.1002/hyp.1344

Moriasi, D.N., Arnold, J.G., Liew, M.W. Van, Bingner, R.L., Harmel, R.D., Veith, T.L., 2007. Model Evaluation Guidelines for Systematic Quantification of Accuracy in Watershed Simulations. Am. Soc. Agric. Biol. Eng. 50, 885–900.

Neitsch, S.L., Arnold, J.G., Williams, J.R., 2011. Soil & Water Assessment Tool Theoretical Documentation.

Ogée, J., Brunet, Y., 2002. A forest floor model for heat and moisture including a litter layer. J. Hydrol. 255, 212–233. doi:10.1016/S0022-1694(01)00515-7

Orth, R., Staudinger, M., Seneviratne, S.I., Seibert, J., Zappa, M., 2015. Does model performance improve with complexity? A case study with three hydrological models. J. Hydrol. 523, 147–159. doi:10.1016/j.jhydrol.2015.01.044

Oudin, L., Andréassian, V., Mathevet, T., Perrin, C., Michel, C., 2006. Dynamic averaging of rainfall-runoff model simulations from complementary model parameterizations. Water Resour. Res. 42, W07410, 1–10. doi:10.1029/2005WR004636

Oudin, L., Hervieu, F., Michel, C., Perrin, C., Andréassian, V., Anctil, F., Loumagne, C., 2005. Which potential evapotranspiration input for a lumped rainfall–runoff model? J. Hydrol. 303, 290–306. doi:10.1016/j.jhydrol.2004.08.026

Pan, F., Zhu, J., Ye, M., Pachepsky, Y. a., Wu, Y.S., 2011. Sensitivity analysis of unsaturated flow and contaminant transport with correlated parameters. J. Hydrol. 397, 238–249. doi:10.1016/j.jhydrol.2010.11.045

Panagoulia, D., 1995. Assessment of daily catchment precipitation in mountainous regions for climate change interpretation. Hydrol. Sci. J. 40, 331–350. doi:10.1080/02626669509491419

Pechlivanidis, I.G., Jackson, B., McMillan, H., Gupta, H. V., 2014. Use of an entropy-based metric in multi-objective calibration to improve model performance. Water Resour. Res. 50, 8066–8083. doi:doi: 10.1002/2013WR014537

Pechlivanidis, I.G., Jackson, B.M., Mcintyre, N.R., Wheater, H.S., 2011. Catchment scale hydrological modelling: a review of model types, calibration approaches and uncertainty analysis methods in the context of recent developments in technology and applications. Glob. NEST J. 13, 193–214.

Perrin, C., Michel, C., Andre, V., 2003. Improvement of a parsimonious model for streamflow simulation. J. Hydrol. 279, 275–289. doi:10.1016/S0022-1694(03)00225-7

Perrin, C., Michel, C., Andre, V., 2001. Does a large number of parameters enhance model performance ? Comparative assessment of common catchment model structures on 429 catchments. J. Hydrol. 242, 275–301.

Pfannerstill, M., Guse, B., Reusser, D., Fohrer, N., 2015. Process verification of a hydrological model using a temporal parameter sensitivity analysis. Hydrol. Earth Syst. Sci. 19, 4365–4376. doi:10.5194/hess-19-4365-2015

Plavšić, J., Blagojević, B., Todorović, A., Despotović, J., 2016. Long-term behaviour of precipitation at three stations in Serbia. Acta Hydrotechnica 29, 23–36.

Pokrajac, D., Stanić, M., 2010. UGROW - the Urban GROundWater modelling system, in: Maksimovic, C., Tejada-Guilbert, A., Zandaryaa, S. (Eds.), Advanced Simulation and Modelling for Urban Groundwater Management - UGROW. UNESCO Publishing, CRC Press, Paris, France, pp. 29–125.

Pomeroy, J.W., Gray, D.M., Hedstrom, N.R., Janowicz, J.R., 2002. Prediction of seasonal snow accumulation in cold climate. Hydrol. Process. 16, 3543–3558. doi:10.1002/hyp.1228

Prohaska, S., Babić Mladenović, M., Stevanović, S., Dimkić, M., Dacić, M., 2009. Vodoprivredna osnova Republike Srbije: hidrometeorološke osnove (Water Resources Development Master Plan). Srbijavode, Belgrade.

Qu, Y., Duffy, C., 2007. A semidiscrete finite volume formulation for multiprocess watershed simulation. Water Resour. Res. 43, W08419. doi:10.1029/2006WR005752

Rakovec, O., Kumar, R., Attinger, S., Samaniego, L., 2016. Improving the realism of hydrologic model functioning through multivariate parameter estimation. Water Resour. Res. 52, 7779–7792.

doi:10.1002/2016WR019430

Refsgaard, J.C., Storm, B., 1995. MIKE SHE, in: Singh, V.P. (Ed.), Computer Models of Watershed Hydrology. Water Resources Publications, Colorado, USA, pp. 809–846.

Sarrazin, F., Pianosi, F., Wagener, T., 2016. Global Sensitivity Analysis of environmental models: Convergence and validation. Environ. Model. Softw. 79, 135–152. doi:10.1016/j.envsoft.2016.02.005

Schaefli, B., Nicótina, L., Imfeld, C., Da Ronco, P., Bertuzzo, E., Rinaldo, A., 2014. SEHR-ECHO v1.0: a Spatially Explicit Hydrologic Response model for ecohydrologic applications. Geosci. Model Dev. 7, 2733–2746. doi:10.5194/gmd-7-2733-2014

Schaap, M.G., Leij, F.J., van Genuchten, M.T., 2001. Rosetta: a Computer Program for Estimating Soil Hydraulic Parameters with Hierarchical Pedotransfer Functions. J. Hydrol. 251, 163–176. doi:10.1016/S0022-1694(01)00466-8

Schoups, G., Vrugt, J.A., Fenicia, F., van de Giesen, N.C., 2010. Corruption of accuracy and efficiency of Markov chain Monte Carlo simulation by inaccurate numerical implementation of conceptual hydrologic models. Water Resour. Res. 46, W10530, 1–12. doi:10.1029/2009WR008648

Schulla, J., 2017. Model Description WaSiM (Water balance Simulation Model). Hydrology Software Consulting J. Schulla, Zürich, Switzerland. [Available at http://www.wasim.ch/downloads/doku/wasim/wasim_2017_en.pdf] (Accessed on 5th March 2018)

Schuurmans, J.M., Bierkens, M.F.P., 2007. Effect of spatial distribution of daily rainfall on interior catchment response of a distributed hydrological model. Hydrol. Earth Syst. Sci. 11, 677–693.

Seibert, J., McDonnell, J.J., 2002. On the dialog between experimentalist and modeler in catchment hydrology: Use of soft data for multicriteria model calibration. Water Resour. Res. 38, 23, 1–14. doi:10.1029/2001WR000978

Seibert, J., Vis, M.J.P., 2012. Teaching hydrological modeling with a user-friendly catchment-runoff-model software package. Hydrol. Earth Syst. Sci. 16, 3315–3325. doi:10.5194/hess-16-3315-2012

Shafii, M., Smedt, F. De, 2009. Multi-objective calibration of a distributed hydrological model (WetSpa) using a genetic algorithm. Hydrol. Earth Syst. Sci. 13, 2137–2149.

Sieber, A., Uhlenbrook, S., 2005. Sensitivity analyses of a distributed catchment model to verify the model structure. J. Hydrol. 310, 216–235. doi:10.1016/j.jhydrol.2005.01.004

Šimůnek, J., Šejna, M., Saito, H., Sakai, M., van Genuchten, M.T., 2009. The HYDRUS-1D Software Package for Simulating the One-Dimensional Movement of Water, Heat, and Multiple Solutes in Variably-Saturated

Media. Department of Environmental Sciences University of California Riverside, Riverside, California.

Stanić, M., Todorović, A., Vasilić, Ž., Plavšić, J., 2017. Extreme flood reconstruction by using the 3DNet platform for hydrological modelling. J. Hydroinformatics jh2017050. doi:10.2166/hydro.2017.050 (in press)

Sulis, M., Paniconi, C., Marrocu, M., Huard, D., Chaumont, D., 2012. Hydrologic response to multimodel climate output using a physically based model of groundwater/surface water interactions. Water Resour. Res. 48, 1–18. doi:10.1029/2012WR012304

Sun, W., Yao, X., Cao, N., Xu, Z., Yu, J., 2016. Integration of soil hydraulic characteristics derived from pedotransfer functions into hydrological models: evaluation of its effects on simulation uncertainty. Hydrol. Res. 1–15. doi:10.2166/nh.2016.150

Thomas, H.A., 1981. Improved Methods for National Water Assessment. U.S. Geological Survey, Cambridge, MA, USA.

Todini, E., 1996. The ARNO rainfall-runoff. J. Hydrol. 175, 339–382.

Todorović, A., Plavšić, J., 2015. Uticaj klimatskih promena na hidrološke režime na slivovima Kolubare, Toplice i Mlave (Climate Change Impact on Hydrologic Regime in the Kolubara, Toplica and Mlava Catchment), in: Ivetić, M., Kapor, R., Plavšić, J. (Eds.), Zbornik radova sa 17. naučnog savetovanja SDHI i SDH održanog 5-6. oktobra 2015. godine u Vršcu. Univerzitet u Beogradu - Građevinski fakultet, pp. 325–340.

Trajkovic, S., 2007. Hargreaves versus Penman-Monteith under Humid Conditions. J. Irrig. Drain. Eng. 133, 38–42. doi:10.1061/(ASCE)0733-9437

Van Der Knijff, J.M., Younis, J., De Roo, A.P.J., 2010. LISFLOOD : A GIS-based distributed model for river basin scale water balance and flood simulation. Int. J. Geogr. Inf. Sci. 24, 189–212. doi:10.1080/13658810802549154

van Esse, W.R., Perrin, C., Booij, M.J., Augustijn, D.C.M., Fenicia, F., Kavetski, D., Lobligeois, F., 2013. The influence of conceptual model structure on model performance: a comparative study for 237 French catchments. Hydrol. Earth Syst. Sci. 17, 4227–4239. doi:10.5194/hess-17-4227-2013

Vasilić, Ž., Stanić, M., Plavsić, J., 2012. Razvoj distribuiranog hidrološkog modela 3DNet-Catch (Development of the 3DNet-Catch Hydrologic Model), in: Zbornik Radova Sa 16. Naučnog Savetovanja Srpskog Društva Za Hidraulička Istraživanja (SDHI) I Srpskog Društva Za Hidrologiju (SDH) Donji Milanovac 2012. Građevinski fakultet u Beogradu, pp. 1–11.

Viviroli, D., Zappa, M., Gurtz, J., Weingartner, R., 2009. An introduction to the hydrological modelling system PREVAH and its pre- and post-processing-tools. Environ. Model. Softw. 24, 1209–1222.

doi:10.1016/j.envsoft.2009.04.001

Wagener, T., Wheater, H.S., Gupta, H.V., 2003. Identification and Evaluation of Watershed Models, in: Calibration of Watershed Models, Water Science and Application, Volume 6. American Geophysical Union, pp. 29–47. doi:10.1029/WS006

Westerberg, I.K., McMillan, H.K., 2015. Uncertainty in hydrological signatures. Hydrol. Earth Syst. Sci. 19, 3951–3968. doi:10.5194/hess-19-3951-2015

Westerberg, I.K., Wagener, T., Coxon, G., McMillan, H.K., Castellarin, A., Montanari, A., Freer, J., 2016. Uncertainty in hydrological signatures for gauged and ungauged catchments. Water Resour. Res. 52, 1847–1865. doi:10.1002/2015WR017635

Wittenberg, H., 1999. Baseflow recession and recharge as nonlinear storage processes. Hydrol. Process. 13, 715–726.

Woolhiser, D.A., Smith, R.E., Goodrich, D.C., 1990. KINEROS, A Kinematic RUnoff and Erosion Model.

Yilmaz, K.K., Gupta, H. V., Wagener, T., 2008. A process-based diagnostic approach to model evaluation: Application to the NWS distributed hydrologic model. Water Resour. Res. 44, W09417, 1–18. doi:10.1029/2007WR006716

Yu, B.B., 1998. Theoretical Justification of SCS Method for Runoff Estimation. J. Irrig. Drain. Eng. 124, 306–310.

Zhang, X., Srinivasan, R., Liew, M. Van, 2009. On the use of multi-algorithm , genetically adaptive multi-objective method for multi-site calibration of the SWAT model. Hydrol. Process. 24, 955–969. doi:10.1002/hyp

List of Figures

Table 1 Stations in the Mlava catchment and data in two simulation periods.

(*Q – mean annual flow, P –annual precipitation and T – mean annual temperature*)

Station	Variable	Elevation (m a.s.l.)	Latitude / Longitude	Available record	Calibration (1993-2003)			Evaluation (2003-2013)		
					min	mean	max	min	mean	max
Veliko Selo	*Q* [m³/s]	92.55*	44 º 30 ’ 21 º 18 ’	1987-2013	3.4	7.2	11.3	5	9.3	16.7
RC Petrovac	*P* [mm]	282	44 º 20 ’	1972-2013	530	707.4	928.5	526.4	693.9	984.7
	T [°C]		21 º 20 ’		10.2	11.8	13.1	11.2	12.1	13.8
Žagubica	*P* [mm]	314	44 º 12 ’	1972-2013	423.8	576	696.9	466.4	683.8	924.8
	T [°C]		21 º 47 ’		8.3	10.1	14.9	10	10.9	12
Crni Vrh	*P* [mm]	1037	44 º 08 ’	1966-2013	635.9	750.1	816.1	661.6	877.2	1134
	T [°C]		21 º 58 ’		5	6.9	8	6.4	7.2	9

* *Zero datum of the staff gauge.*

1291 **Table 2** Flow-related hydrological signatures considered for the model evaluation.

Label	Signature	Description
Q_{MEAN}	Mean flow (m^3/s)	Mean flow in the simulation period (m^3/s); indicates model ability to reproduce long-term water balance.
C_V	Flow variability	The coefficient of variation of daily flows; reflects agreement in flow dynamics.
AC	Autocorrelation coefficient	1-day autocorrelation coefficient of daily flows. Related to flow dynamics/flashiness: large catchments show high autocorrelation, while autocorrelation is small in flashy catchments.
KGE_{FDC}	*KGE* of the entire FDC	*KGE* calculated from the entire FDC.
KGE_{HF}	*KGE* of the high-flow FDC segment	*KGE* calculated from the high flows (exceedance probabilities from 0 to 0.05). Related to soil moisture redistribution.
KGE_{MF}	*KGE* of the mid-flow FDC segment	*KGE* calculated from the log-transformed flows (exceedance probabilities between 0.2 and 0.7). Related to soil moisture redistribution.
KGE_{LF}	*KGE* of the low-flow FDC segment	*KGE* calculated from the log-transformed flows (exceedance probabilities between 0.7 and 1). Indicates model ability to reproduce baseflow.
$Q_{1\%}$, $Q_{5\%}$, $Q_{95\%}$, $Q_{99\%}$	Flow percentiles (m^3/s)	Characteristic percentiles of daily flows representing extremely high ($Q_{1\%}$, $Q_{5\%}$) and low flows ($Q_{95\%}$, $Q_{99\%}$). Indicate model ability to reproduce extreme flows.

1292

Table 3 Hydrological signatures of the observed and simulated flows. The signatures calculated from the ensemble are represented by the 2.5th, 50th and 97.5th percentiles.

Hydrologic signature	Calibration (1993-2003)				Evaluation (2003-2013)			
	Observed	Simulated			Observed	Simulated		
		2.5	50	97.5		2.5	50	97.5
Q_{MEAN}	7.22	6.25	7.08	8.06	9.03	8.10	9.62	10.73
C_V	1.46	1.18	1.41	1.62	1.44	1.26	1.52	1.70
AC	0.863	0.852	0.920	0.955	0.92	0.881	0.940	0.967
KGE_{FDC}	/	0.82	0.90	0.97	/	0.72	0.84	0.97
KGE_{HF}	/	0.43	0.59	0.85	/	0.57	0.81	0.94
KGE_{MF}	/	0.40	0.72	0.93	/	0.19	0.69	0.96
KGE_{LF}	/	-0.01	0.41	0.81	/	-0.01	0.48	0.80
$Q_{1\%}$	1.1	0.01	0.33	1.07	1.07	0.04	0.33	1.11
$Q_{5\%}$	1.2	0.08	0.52	1.45	1.3	0.11	0.64	1.60
$Q_{95\%}$	22.29	22.91	27.35	31.59	33.1	31.42	37.60	43.63
$Q_{99\%}$	55.1	42.43	49.82	56.90	67.56	57.39	72.00	81.62

Figure1

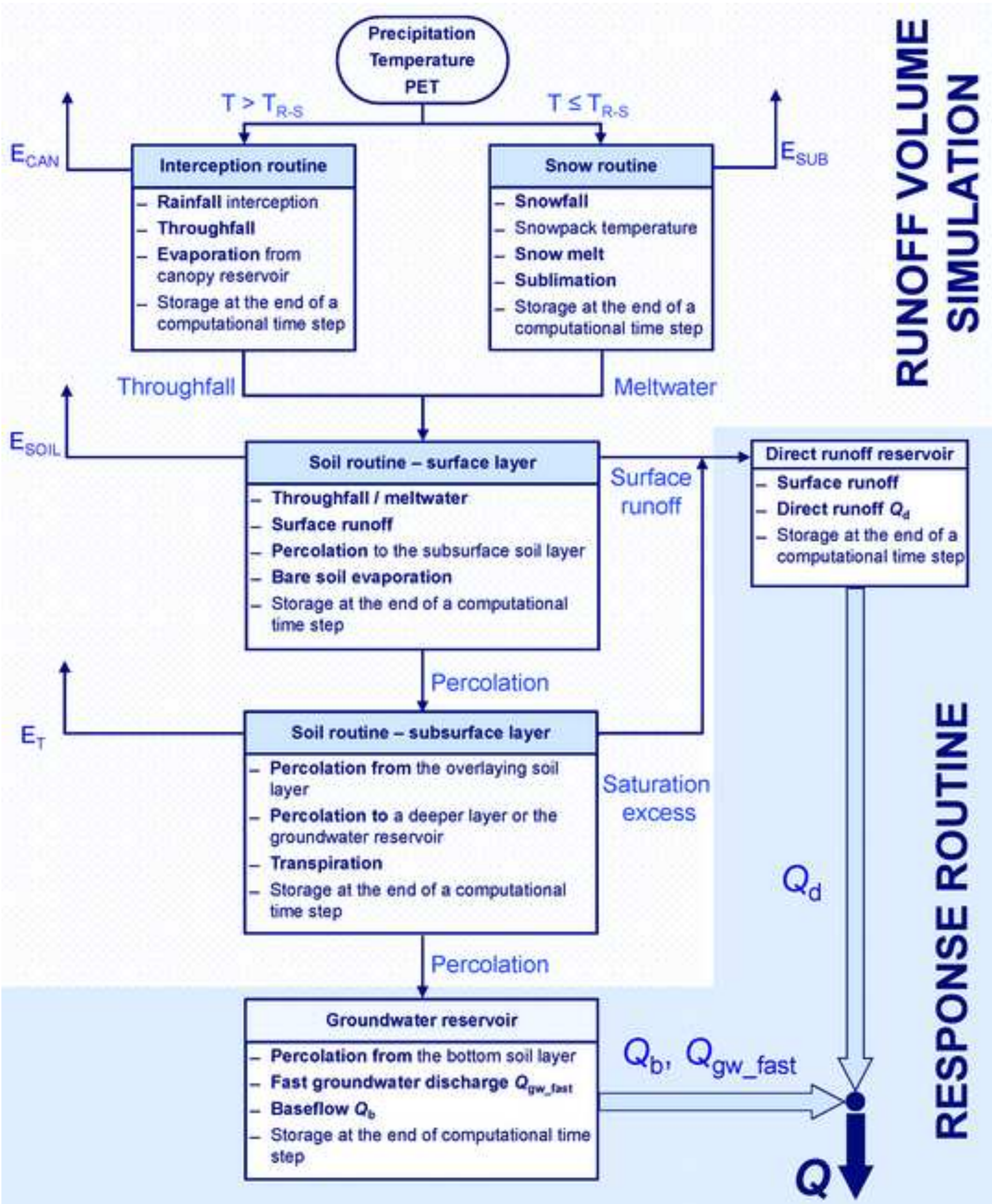
Precipitation
Temperature
PET
T > T_R-S
T ≤ T_R-S
E_CAN
Interception routine
– Rainfall interception
– Throughfall
– Evaporation from canopy reservoir
– Storage at the end of a computational time step
Snow routine
– Snowfall
– Snowpack temperature
– Snow melt
– Sublimation
– Storage at the end of a computational time step
E_SUB
RUNOFF VOLUME SIMULATION
Throughfall
Meltwater
E_SOIL
Soil routine – surface layer
– Throughfall / meltwater
– Surface runoff
– Percolation to the subsurface soil layer
– Bare soil evaporation
– Storage at the end of a computational time step
Surface runoff
Direct runoff reservoir
– Surface runoff
– Direct runoff Q_d
– Storage at the end of a computational time step
Percolation
E_T
Soil routine – subsurface layer
– Percolation from the overlaying soil layer
– Percolation to a deeper layer or the groundwater reservoir
– Transpiration
– Storage at the end of a computational time step
Saturation excess
Q_d
RESPONSE ROUTINE
Percolation
Groundwater reservoir
– Percolation from the bottom soil layer
– Fast groundwater discharge Q_gw_fast
– Baseflow Q_b
– Storage at the end of computational time step
Q_b, Q_gw_fast
Q

Figure2

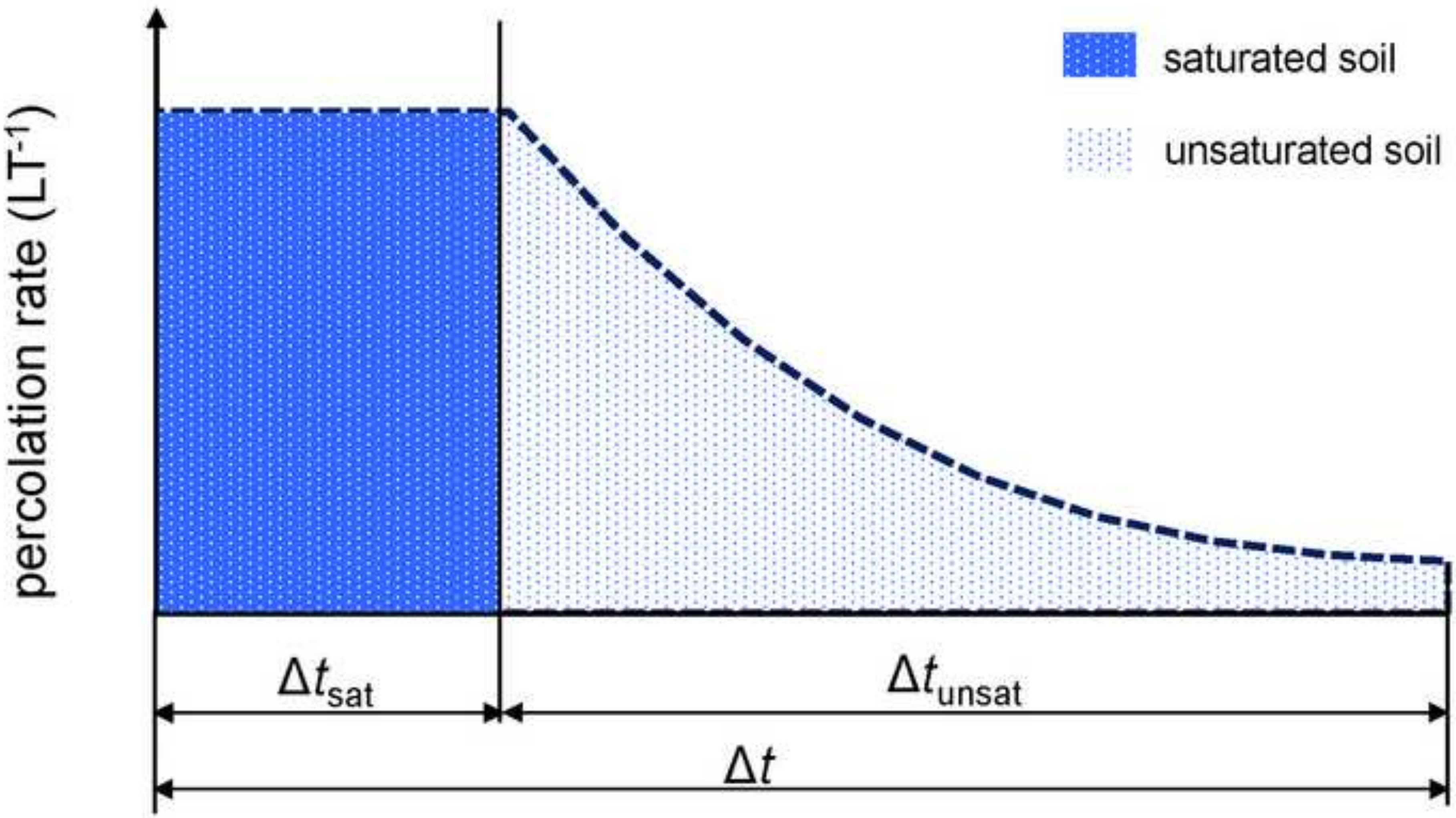

percolation rate (LT^{-1})
saturated soil
unsaturated soil
Δt_{sat}
Δt_{unsat}
Δt

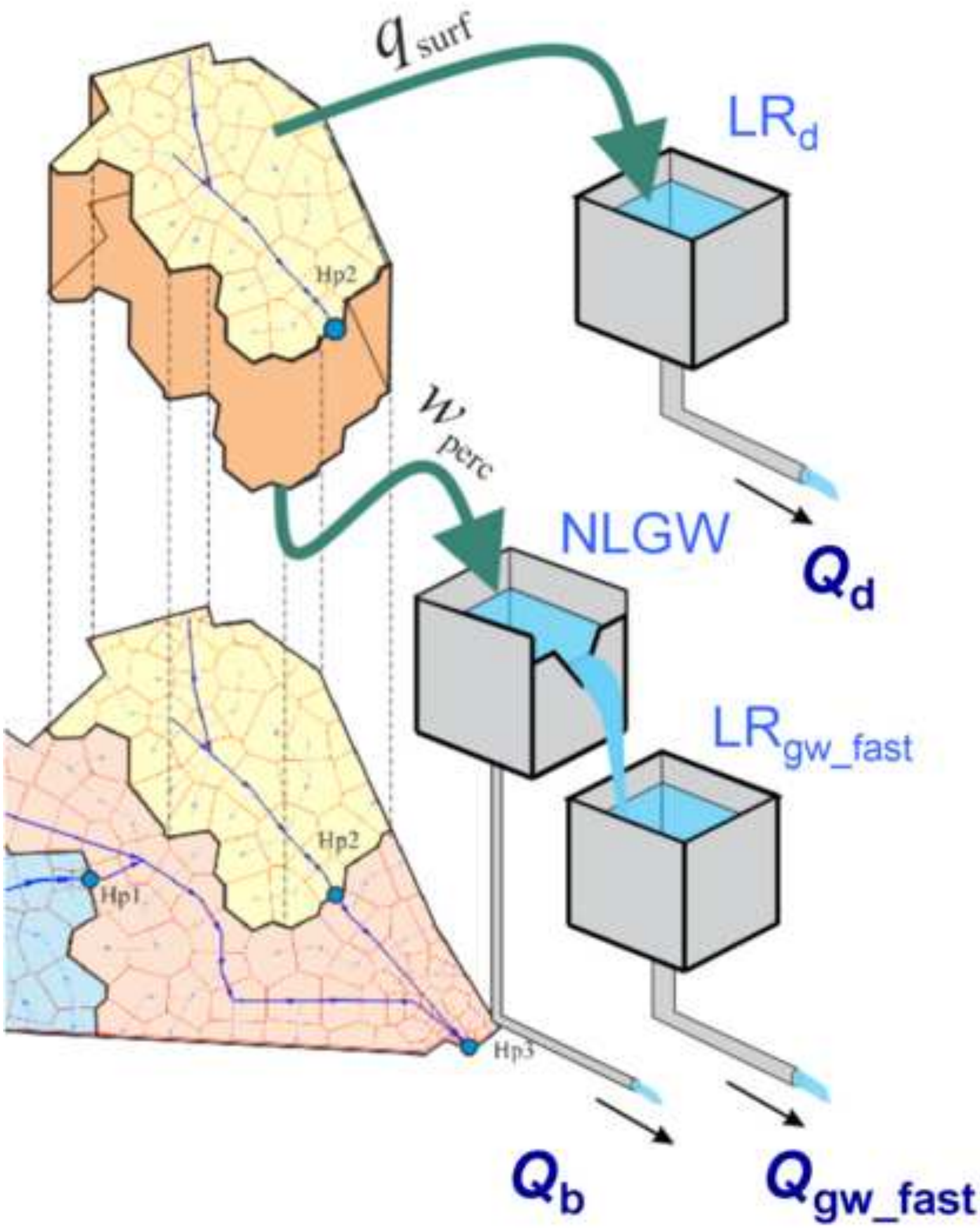

LRd – linear reservoir for surface runoff routing

NLGW – nonlinear groundwater reservoir

LRgw_fast – linear reservoir for fast groundwater discharge routing

Qd – direct runoff

Qgw_fast – fast groundwater discharge

Qb – baseflow

qsurf – surface runoff

wperc – percolation from the deepest soil layer

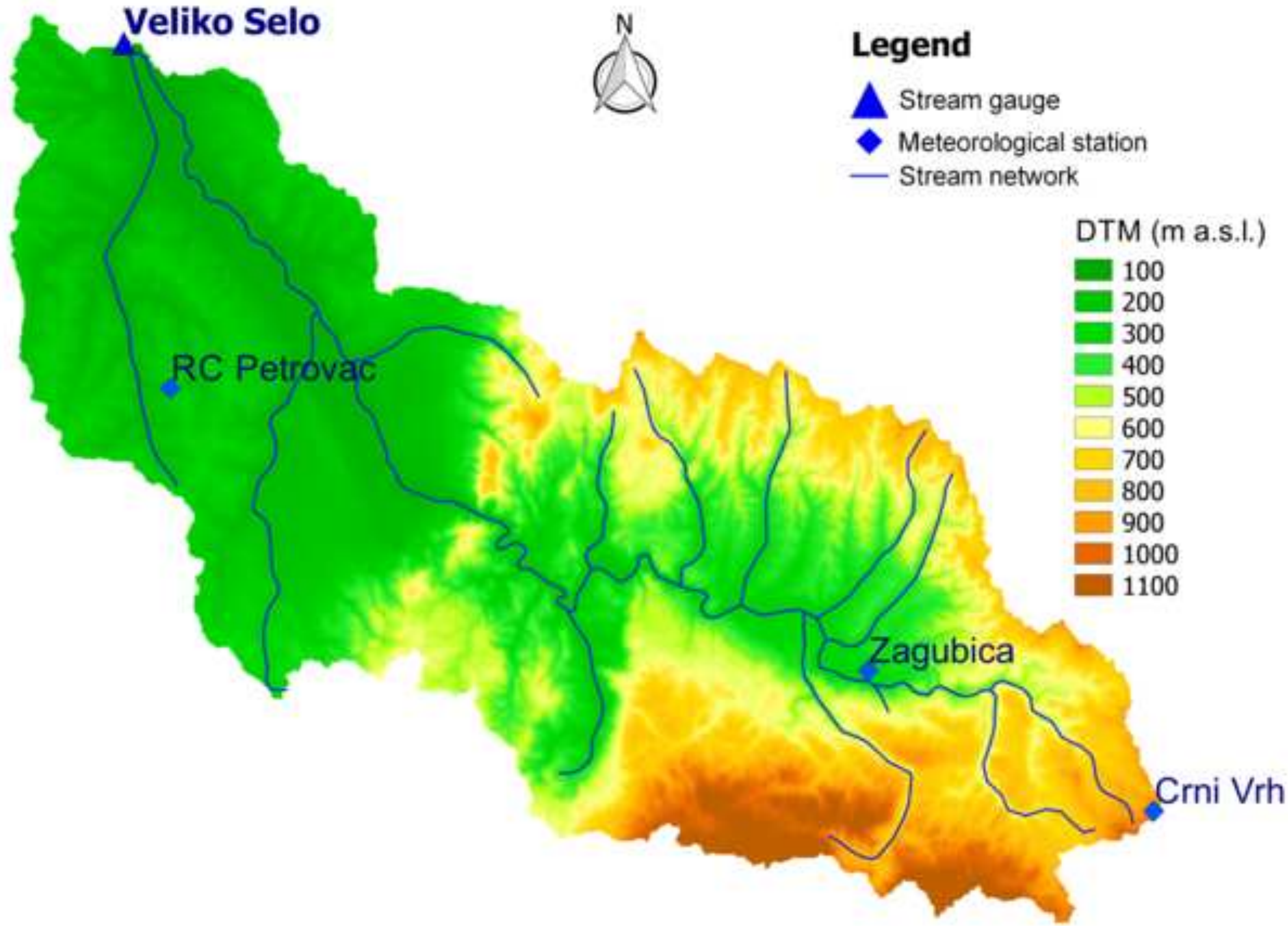
Veliko Selo
N
Legend
Stream gauge
Meteorological station
Stream network
DTM (m a.s.l.)
100
200
300
400
500
600
700
800
900
1000
1100
RC Petrovac
Zagubica
Crni Vrh

Figure5
Click here to download high resolution image

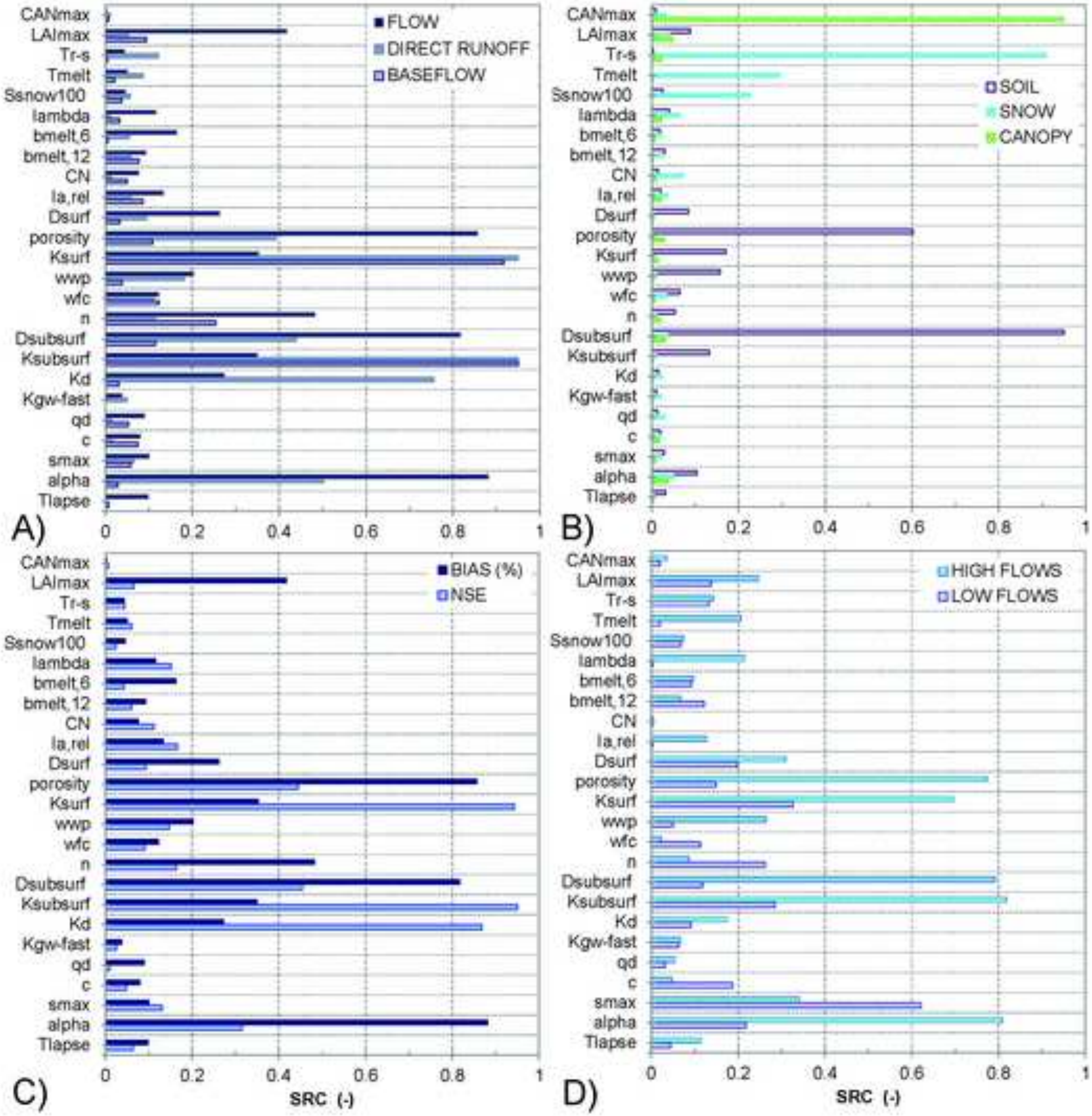

Figure6

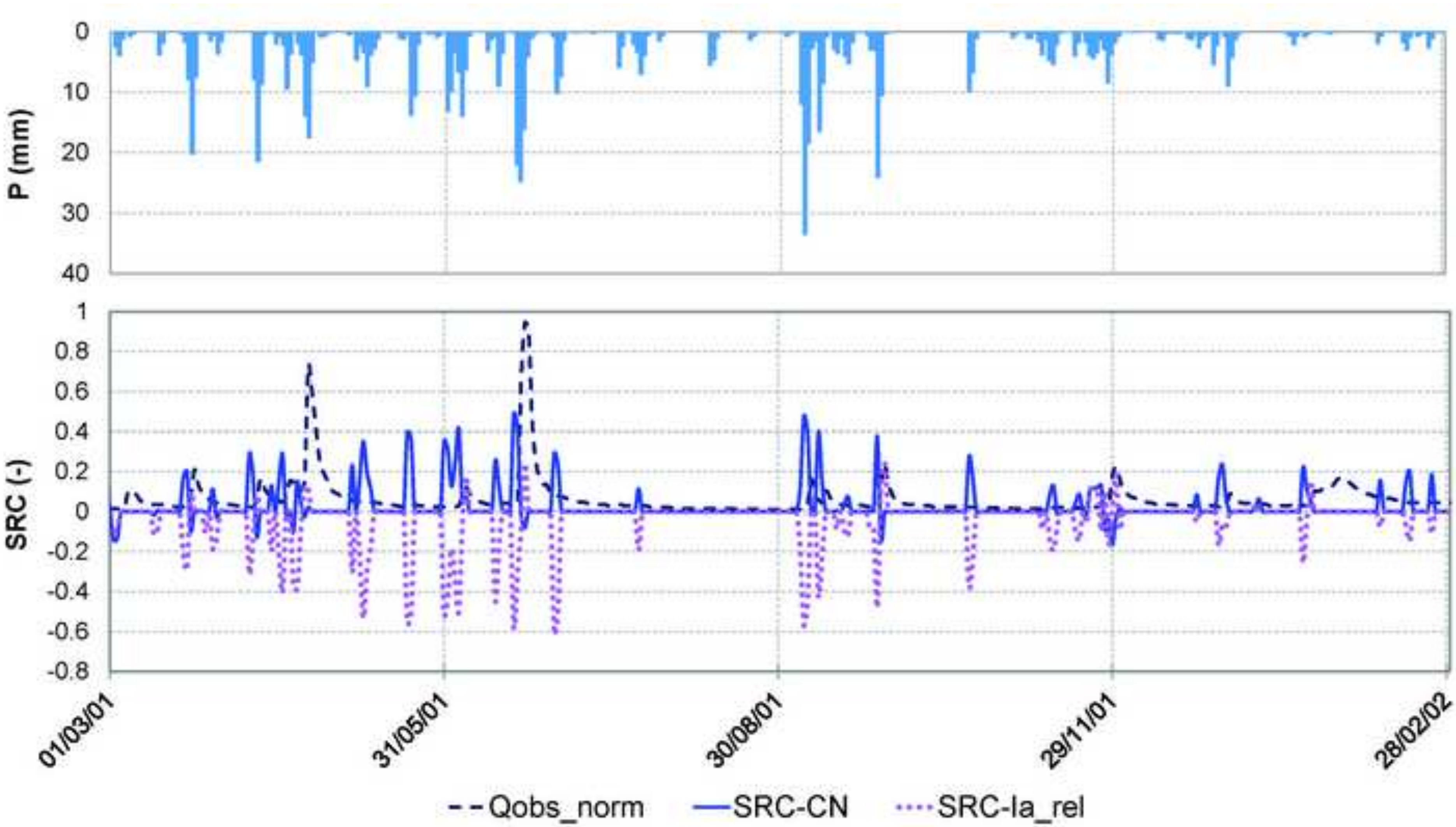

P (mm)
0
10
20
30
40
SRC (-)
1
0.8
0.6
0.4
0.2
0
-0.2
-0.4
-0.6
-0.8
01/03/01
31/05/01
30/08/01
29/11/01
28/02/02
Qobs_norm
SRC-CN
SRC-Ia_rel

Figure7

Click here to download high resolution image

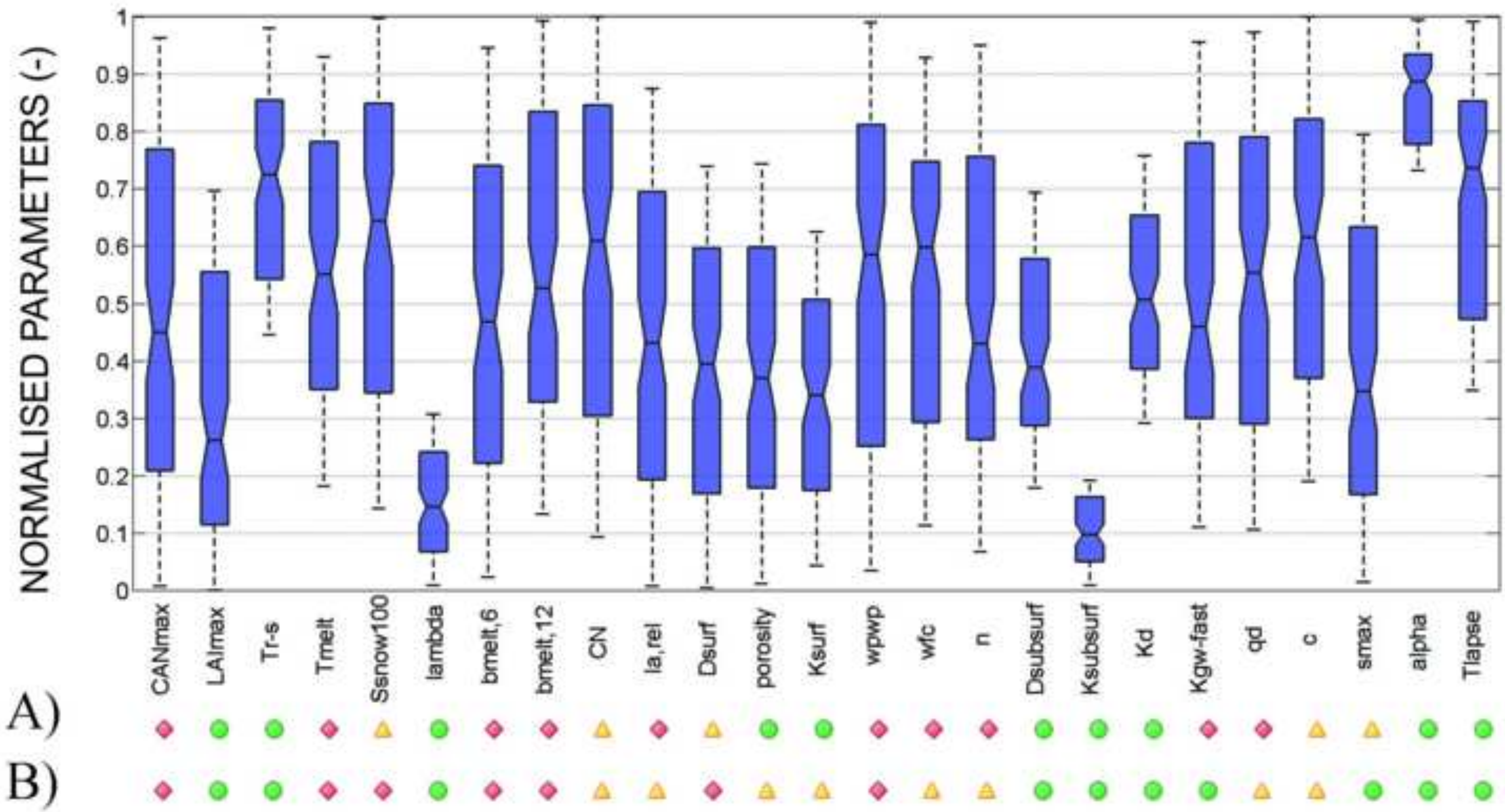

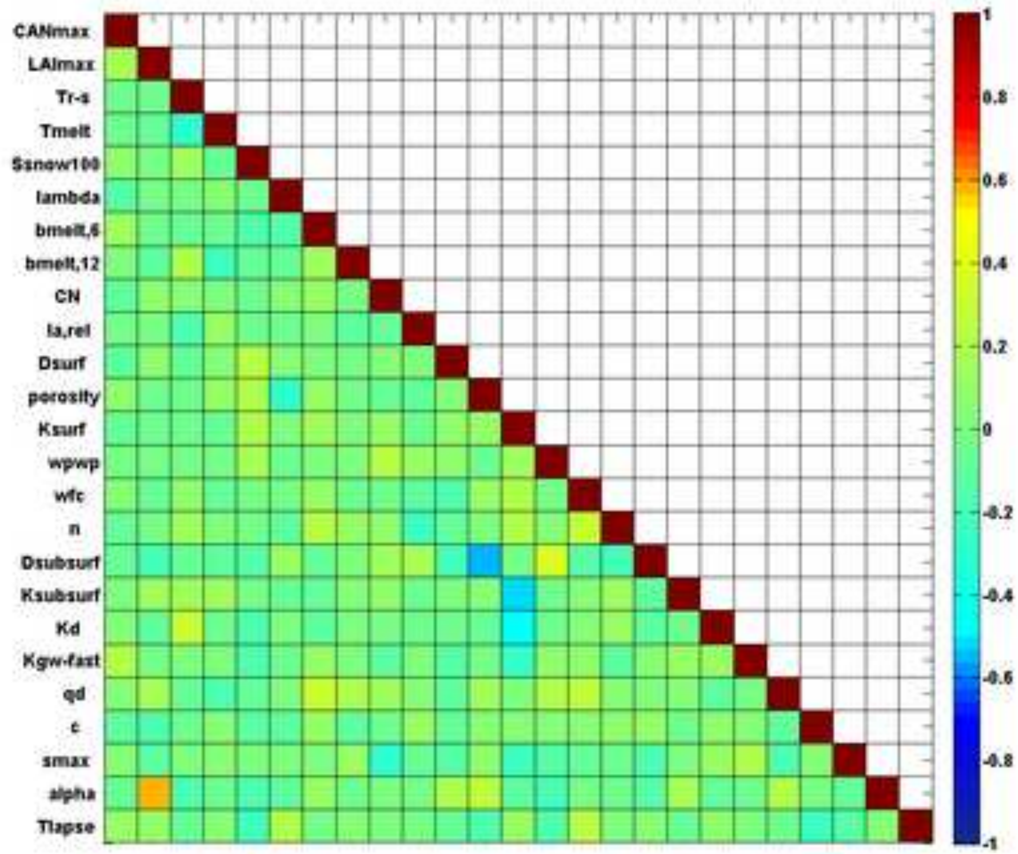
CANmax
LAImax
Tr-s
Tmelt
Ssnow100
lambda
bmelt,6
bmelt,12
CN
la,rel
Dsurf
porosity
Ksurf
wpwp
wfc
n
Dsubsurf
Ksubsurf
Kd
Kgw-fast
qd
c
smax
alpha
Tlapse
1
0.8
0.6
0.4
0.2
0
-0.2
-0.4
-0.6
-0.8
-1

Figure9

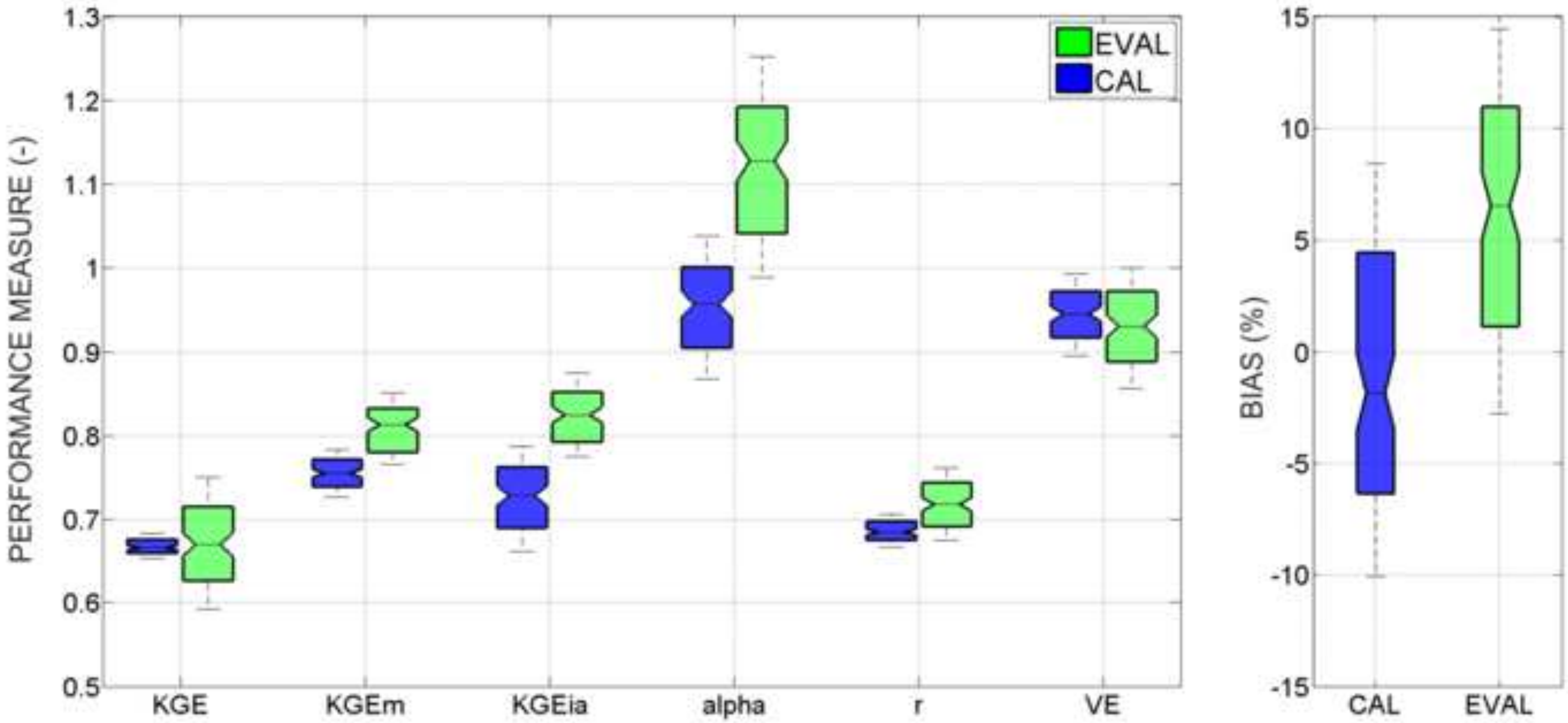

PERFORMANCE MEASURE (-)
1.3
1.2
1.1
1
0.9
0.8
0.7
0.6
0.5
EVAL
CAL
KGE
KGEm
KGEia
alpha
r
VE
BIAS (%)
15
10
5
0
-5
-10
-15
CAL
EVAL

Figure10

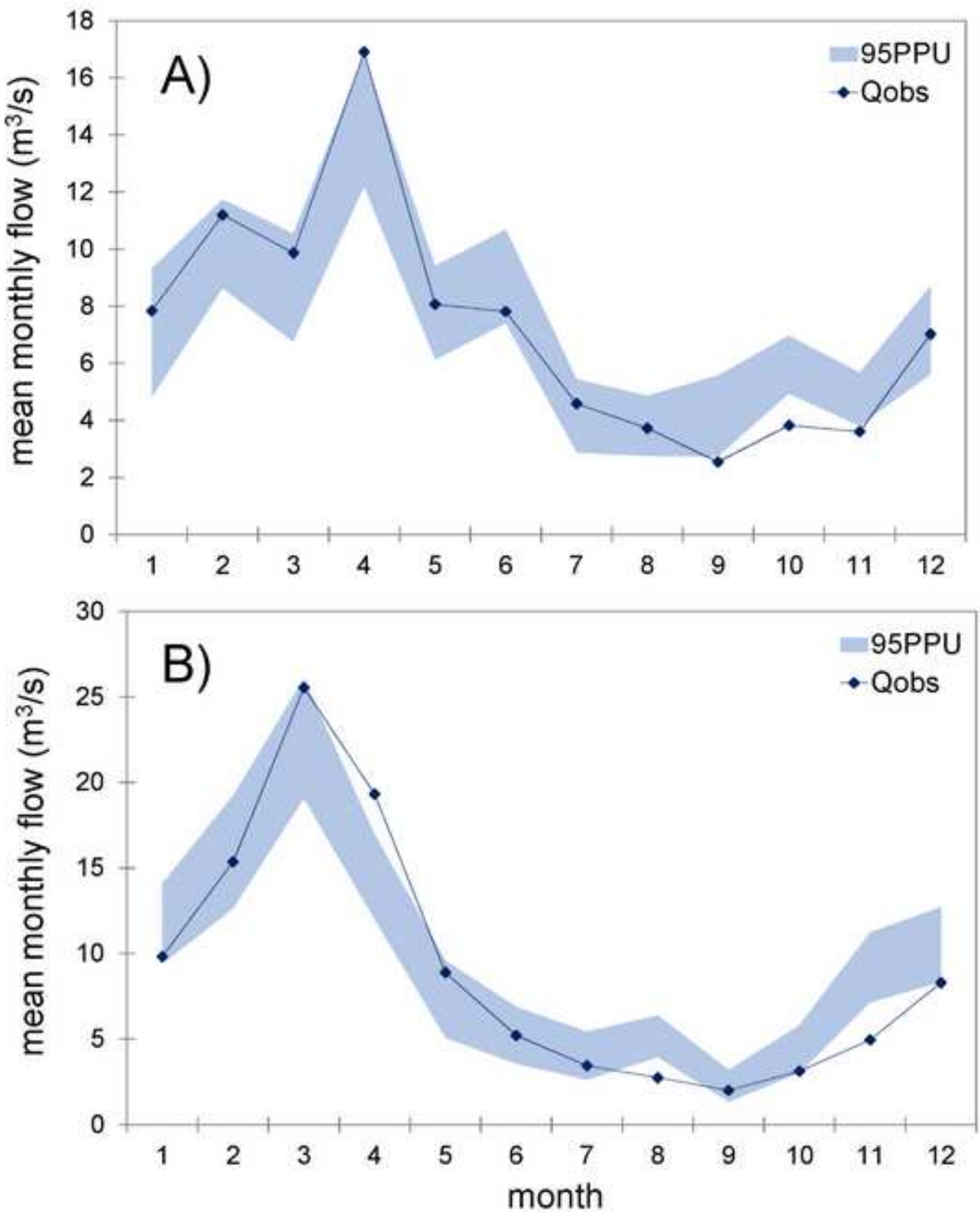

A)
95PPU
Qobs
mean monthly flow (m3/s)
0
2
4
6
8
10
12
14
16
18
1
2
3
4
5
6
7
8
9
10
11
12
B)
95PPU
Qobs
mean monthly flow (m3/s)
0
5
10
15
20
25
30
1
2
3
4
5
6
7
8
9
10
11
12
month

Figure11

Click here to download high resolution image

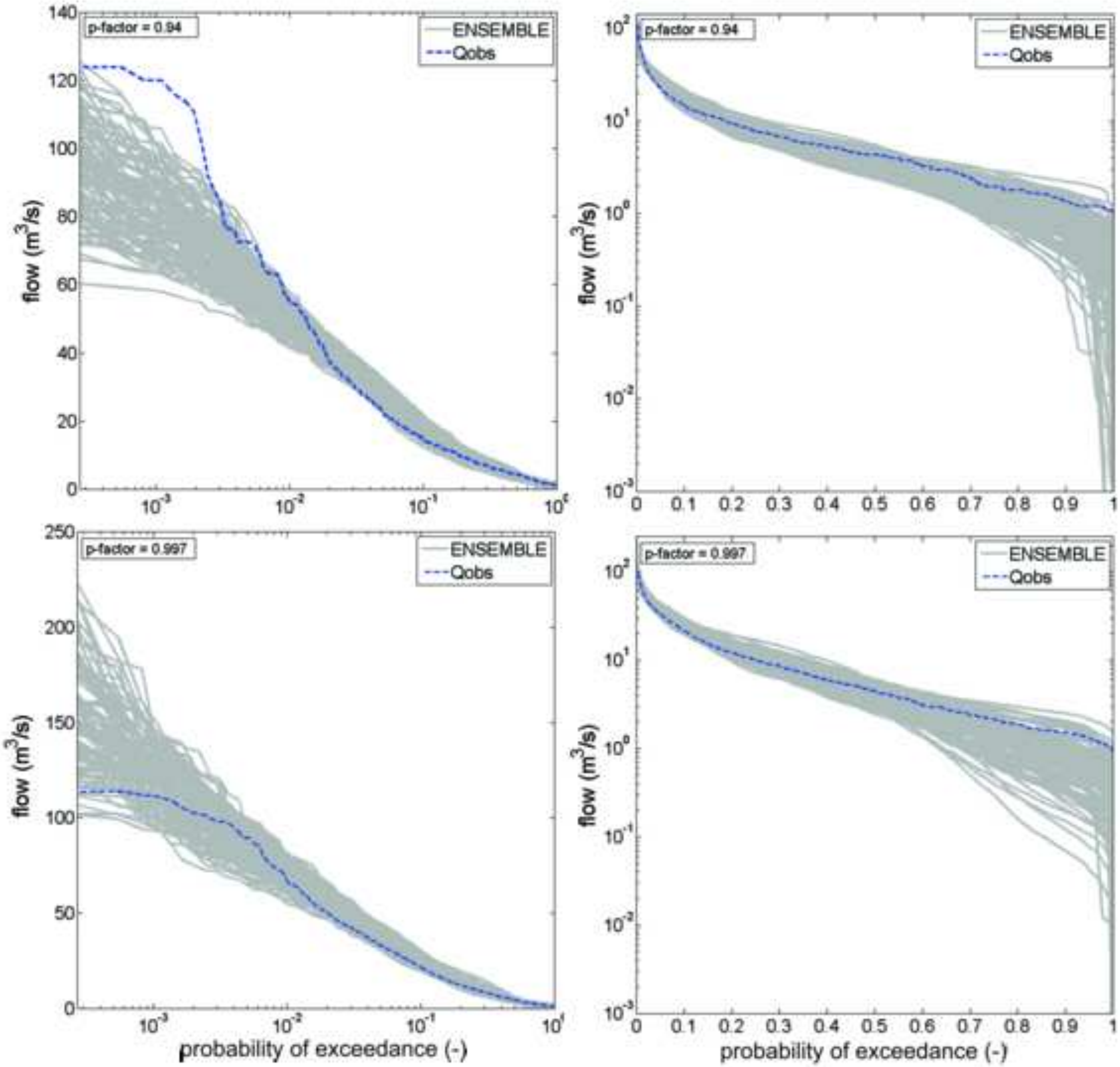

Figure12

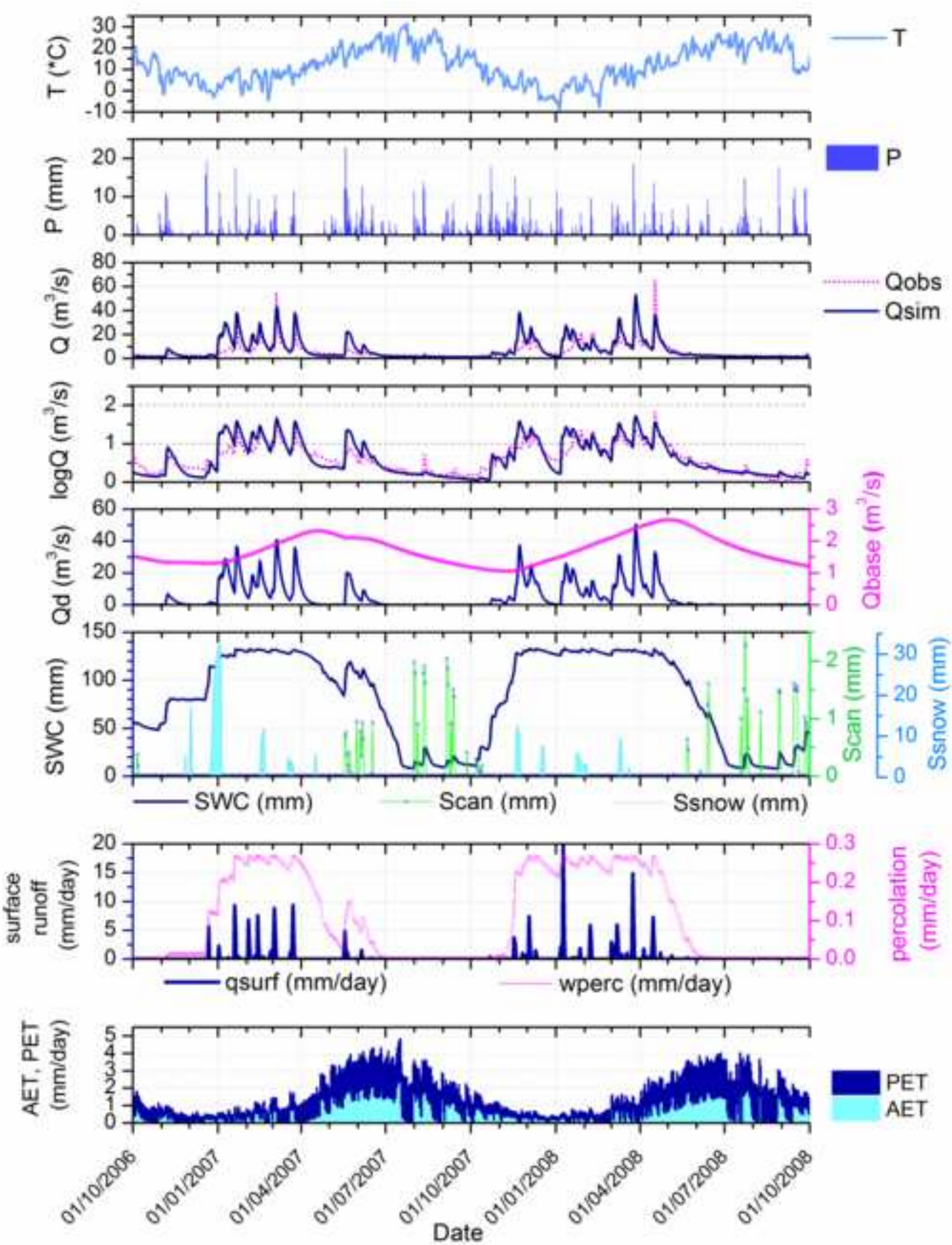

T (°C)
T
P (mm)
P
Q (m³/s)
Qobs
Qsim
logQ (m³/s)
Qd (m³/s)
Qbase (m³/s)
SWC (mm)
Scan (mm)
Ssnow (mm)
SWC (mm)
Scan (mm)
Ssnow (mm)
surface runoff (mm/day)
percolation (mm/day)
qsurf (mm/day)
wperc (mm/day)
AET, PET (mm/day)
PET
AET
01/10/2006
01/01/2007
01/04/2007
01/07/2007
01/10/2007
01/01/2008
01/04/2008
01/07/2008
01/10/2008
Date

HIGHLIGHTS FOR THE ARTICLE:

The 3DNet-Catch Hydrologic Model: Development and Evaluation

Andrijana Todorović[a*], Miloš Stanić[a], Željko Vasilić[a], Jasna Plavšić[a]

[a] University of Belgrade, Faculty of Civil Engineering, Bulevar kralja Aleksandra 73, Belgrade, Serbia

[*] Corresponding author, e-mail: *atodorovic@grf.bg.ac.rs*

- 3DNet-Catch provides balanced model complexity and adaptability to local conditions
- 3DNet-Catch includes the interception, snow, soil, and runoff and channel routing
- A comprehensive evaluation of model parameterisation and performance is conducted
- Most model parameters are physically meaningful, well-identifiable and uncorrelated
- Consistently good performance despite input data from sparse meteorological network